

2175:81823

m823

Stanford Public Library

TECHNICAL MEMORANDUMS
NATIONAL ADVISORY COMMITTEE FOR AERONAUTICS

No. 823

EXPERIMENTAL INVESTIGATION OF THE PROBLEM
OF SURFACE ROUGHNESS

By H. Schlichting

Ingenieur-Archiv
Vol. VII, No. 1, February 1936

Washington
April 1937



NATIONAL ADVISORY COMMITTEE FOR AERONAUTICS

TECHNICAL MEMORANDUM NO. 823

EXPERIMENTAL INVESTIGATION OF THE PROBLEM OF
SURFACE ROUGHNESS*

By H. Schlichting

INTRODUCTION

As a result of numerous recent investigations (references 1-6), we are now sufficiently well acquainted, from an experimental viewpoint, with the laws of turbulent flow in smooth pipes, channels, and along smooth plates. Laws of general applicability have been found for the velocity distribution and the frictional resistance, and with the aid of these we are now in a position to handle the problem of turbulent flow for any cases of velocities and dimensions that may arise in practice.

As far as turbulent flow in rough pipes and channels and along rough plates is concerned, and this type of flow is of greater practical interest than that along smooth walls, we are likewise in possession of extensive test results accumulated within the past few years - which results only very recently, however, have been evaluated so as to yield a few laws of general applicability.

On account of the considerable importance of the problem of surface roughness in the solution of many problems of engineering, the gathering of further test data on the frictional drag is urgently necessary. In what follows will be presented a new experimental method which, with the aid of the generally applicable laws that have already been found, enables surface roughness tests to be carried out in a very simple manner and the results to be directly applied to practical cases.

In the formulation of the universal law of velocity distribution at a smooth or rough wall, it was found very useful to introduce a nondimensional velocity $\varphi = u/v_*$ and a nondimensional distance from the wall $\eta = yv_*/v$

* "Experimentelle Untersuchungen zum Rauheitsproblem." Ingenieur-Archiv, vol. VII, no. 1, February 1936, pp. 1-34.

(reference 2) where u denotes the velocity, y the distance from the wall, and $v_* = \sqrt{\tau/\rho}$ is a velocity computed from the shearing stress τ at the wall and may be denoted as the "shearing stress velocity," ρ is the density, and ν the kinematic viscosity.

The extensive test results of J. Nikuradse (reference 6) on the velocity distribution in smooth pipes have shown that the nondimensional velocity thus formed is always the same function of the nondimensional distance from the wall $\varphi = \varphi(\eta)$, the plot of φ against $\log \eta$ being a straight line:

$$\text{or } \left. \begin{aligned} \varphi &= A + B \log \eta = 5.5 + 5.75 \log \eta \\ \frac{u}{v_*} &= 5.5 + 5.75 \log \frac{y v_*}{\nu} \end{aligned} \right\} \text{ (smooth) } \quad (1)$$

Theoretical considerations (reference 3) show that this straight-line law may be expected to hold if the effect of the viscosity on the turbulence is vanishingly small. It may therefore be assumed that equation (1) remains valid up to the highest attainable Reynolds Numbers. The velocity-distribution law (1) is a so-called boundary-wall law; that is, the velocity in the neighborhood of the wall depends, besides on the viscosity and density, only on the distance from the wall and on the shear stress at the wall, but it is not influenced by any process occurring at some great distance from the position under consideration, in the pipe or channel; for example, not on the relations existing at the other wall. (This fact is taken into account in applying the results of pipe and channel tests to towed plates.) Conversely, given the known values of u , y , ρ , and ν , the shear stress τ at the wall may be computed from the velocity-distribution law, a fact which we shall make use of in the carrying out of the tests.

The frictional resistance law is closely connected, as we know, with the velocity-distribution law and is found to be

$$\frac{1}{\sqrt{\lambda}} = 2 \log (\text{Re} \sqrt{\lambda}) - 0.8 \quad \text{(smooth)} \quad (2)$$

where $\lambda = \frac{dp}{dx} \frac{2d}{\rho \bar{u}^2}$ is the friction factor and $\text{Re} = \frac{\bar{u}d}{\nu}$ is the Reynolds Number. This law has the same range of

application as the velocity-distribution law (1) and therefore likewise applies to arbitrarily high Reynolds Numbers.

If we plot similarly the relation $\phi = f(\log \eta)$ for rough pipes, then from the measurements of Nikuradse (reference 10) on pipes artificially roughened with sand, a straight line is obtained for the velocity distribution for each value of relative roughness k/r (k = absolute roughness, r = pipe radius) and each Reynolds Number. It is found, in particular, that all the straight lines run parallel, the common slope $B = 5.75$ being the same as for the smooth pipe. Using the identity

$$\frac{yv^*}{v} = \frac{y}{k} \frac{v_*k}{v}$$

the universal velocity-distribution law for rough pipes may therefore also be written in the form

$$\phi = A + 5.75 \log \frac{y}{k}, \quad A = A \left(\frac{v_*k}{v} \right) \quad (\text{rough}) \quad (3)$$

According to the measurements of Nikuradse the magnitude of A depends only on the number v_*k/v , involving the "shear stress velocity" v_* , the roughness k , and the kinematic viscosity ν . From equation (3) the resistance law for a rough wall is obtained as

$$\lambda = (2 \log \frac{r}{k} + a)^{-2} \quad (\text{rough}) \quad (4)$$

where a similarly depends on v_*k/v .

The velocity-distribution and resistance laws (3) and (4) for rough walls were extensively investigated by Nikuradse, whose object it was to investigate a certain simple type of roughness over a very large range of Reynolds Numbers. The roughness chosen was sand of grain sizes $k_s = 0.8; 0.4; 0.2$, and 0.1 millimeter, the sand being glued on as densely as possible to the inner surface of brass pipes of various diameters ($d = 2.5, 5$, and 10 cm) by means of lacquer. The greatest relative roughness was therefore, $r/k_s = 15$, and the smallest, $r/k_s = 500$. Figure 1 shows the dependence thus found of the resistance or friction factor λ on the Reynolds Number $Re = \frac{\bar{u}d}{\nu}$ and the relative roughness r/k_s , $\lambda = f(Re, r/k_s)$, for a

range of Reynolds Numbers from 10^3 to 10^6 . It may be seen that for the friction factor three different regions may be made out which may be characterized as follows:

In region I, that for small Reynolds Numbers, the resistance of the rough pipe is equal to that of the smooth one. The roughness elements lie entirely within the very thin laminar layer which in turbulent flow adheres quite close to the wall (laminar sub-layer).

In region II (region of transition) the resistance increases with increasing Reynolds Number. The thickness of the laminar layer is of the same order of magnitude as the height of the roughness, so that with increasing Reynolds Number (that is, with decreasing thickness of the laminar layer) more of the roughness excrescences protrude through the layer and therefore the resistance strongly increases.

In region III the resistance factor is independent of the Reynolds Number and depends only on the relative roughness. All the roughness elements protrude through the laminar layer and the flow may now be considered entirely as turbulent flow. For λ we then have the simple formula

$$\lambda = \left(1.74 + 2 \log \frac{r}{k_s} \right)^{-2} \quad (5)$$

The velocity-distribution law (3) likewise assumes a particularly simple form for region III since A also becomes independent of $v_* k/v$. For the special case of the sand roughness of Nikuradse, $A = A_s = 8.48$ in this region.

The three regions thus made out apply not only to the sand roughness but also to many other kinds of roughness met with in practice. The region III where the flow may be considered as entirely turbulent is the most important, and our investigation will be mainly concerned with this region.

The universally applicable laws for smooth and rough walls we have just considered, enable us to carry out roughness tests in a particularly simple manner as will be described below. The idea suggests itself of establishing a "standard roughness" to which any arbitrary roughness may

be referred for comparison. Such a standard would naturally be quite arbitrary and the choice would depend on practical considerations. We shall not, however, consider this subject further here. Without setting up any standard roughness the problem in any practical case where roughness must be taken into account may be considered as completely solved if it is possible to indicate the resistance for any kind of roughness both for the case of pipe and channel flow and for a plate towed in a region of unconfined flow - the latter case being of fundamental importance in the study of ship hull design. In both cases a necessary requirement is that it should be possible to extend the results directly to pipes and channels or plates of other dimensions. It should be possible for any given geometric form of the roughness, to compute the frictional resistance theoretically, although such computation would rarely succeed in giving the required accuracy. It is all the more important therefore that we be in possession of a simple experimental method whereby, without any undue time expenditure, any practical problem involving surface roughness that may occur in practice, may be investigated to order, so to speak. An apparatus of a simple type has been developed in Göttingen and has the form of a rectangular channel with three smooth walls and one interchangeable rough wall. This apparatus is found to be particularly useful for ship-design problems, since by a simple extension of the results obtained in this channel, they may be directly applied to the case of a towed plate. In this manner the plate-towing tests that in many cases involve elaborate testing and much time and money expenditure, may be dispensed with.

In order to have the characteristics of the new experimental procedure clearly brought out and at the same time to obtain some further results on the nature of flow in rough pipes and channels, we have investigated a series of uniform, geometrically similar, simple types of roughness.

In the tests of Nikuradse the roughness was characterized by a single parameter, namely, the absolute roughness $k = k_s =$ size of sand grain. On account of the varied character of the types of roughness that may come up in practice, it will not be found possible, in most cases, to use a single parameter but at least one more will be found necessary, namely, the roughness density, which is the number of individual roughness elements per unit of area. (In the Nikuradse tests the roughness density had a constant value near the maximum.) It is therefore also

necessary to investigate how, for a similar geometrical form, the frictional resistance depends on the density of the roughness, and this question we shall likewise consider in the tests described below.

I. DESCRIPTION OF TESTS

Test Set-Up

The tests were conducted on the test set-up shown in figures 2, 3, and 4. This is essentially the same as that previously employed by Nikuradse in his tests on smooth and rough pipes. A detailed description of the entire set-up is given in the V.D.I., Forschungsheft 256 (reference 6), so that we need here only consider wherein our apparatus differs from his.

The centrifugal pump *kp* delivers the water from the stored water channel *vk* into the water tank *wk*. From the latter the water flows through the pipe *zr* and the starting run channel *ak*, and reaches the channel *mk* where the measurements are taken and then flows through the velocity-measuring apparatus *gm* back into the stored water channel *vk*. The channel on which measurements are taken is more clearly shown in figure 4. It consists of two parts, each 3.20 meters long, screwed to each other at the flanges. Both channels have the same cross section 4.0 by 17.0 centimeters. The actual measurements are made at the rear portion, the forward portion serving as a take-off run. The walls of the latter portion are smooth. This take-off channel, which originally was intended as a measuring channel, was welded together of U beams and sheet iron. The latter method of construction turned out to be too inaccurate, however, since, for reliable results to be obtained, it is necessary that the height of the channel along its entire length should not vary by more than 1/10 millimeter (see below). The second channel was therefore constructed of cast steel and consists of two parts: 1 - a rectangular open run with smooth walls and grooves at the sides, in which the test plate is fitted; and 2 - a cover which is placed above the test plate and is tightly screwed onto the lower half of the channel (fig. 4). To obtain sufficient tightness between cover and test plate a linen packing sprinkled with red oxide of lead was placed between cover and test plate. By careful workmanship of the walls and side grooves at the lower half of

the channel, uniformity in the height of the channel all along the channel length was achieved. As a protection against rust and to attain sufficient smoothness of the walls, the inside of the channel was spread over with "inertol" and rubbed smooth with sandpaper. The very slight roughnesses that still remained do not enter into the results as errors but are taken into account in the evaluation of the results by the method described below. The wall thus treated may practically be considered as hydraulically smooth.

At eight positions along the smooth wall, 40 centimeters apart, the static pressure was taken. At each section three orifices were bored so as to balance out any small errors at each section by taking an average. At each section at which the static pressure was taken, the channel was provided with small windows through which the flow could be observed. It was also possible to insert a pitot tube through an orifice in the smooth wall so that the velocity distribution could be measured at various sections of the channel. With the aid of a block and pulley arranged above the channel cover, the latter could easily be lifted up after unloosening the screws, and the test plate interchanged with another.

Types of Roughness Elements Used

The test plates upon which the roughness was to be investigated were of such dimensions as to fit accurately into the channel, their lengths being 320 centimeters and width 17.8 centimeters, of which 5 millimeters were allowed on each side for fitting into the side grooves. These plates were of sheet metal 5 millimeters thick, on which was placed square bar iron of 15 millimeters thickness, so that the total plate thickness was 20 millimeters. Care was taken to see that the plates were very even.

Table I gives the data on all the rough plates investigated, and figure 6 shows the appearance of each plate. Six groups of roughness elements were used, and each group at several roughness densities. The dimensions and arrangement of these roughness elements are indicated on figure 5: I, spheres, diameter $d = 0.41$ cm; II, spheres, diameter $d = 0.21$; III, spherical segments; IV, cones; V, "short angles"; VI, "long angles"; and in addition, a plate with "Hamburg sand" of a mean grain size $k = 1.35$. This is the same sand that was employed by G. Kempf (reference 17) in his towing tests on rough plates. In the preliminary tests

the same kind of sand was employed as that used by Nikuradse in his tests on pipes. To prepare a sand plate the plate which was at first well smoothed, was sprayed with "inertol" and the sand was spread directly over it, the lower sand layer strongly adhering to the plate. After shaking off the excess sand the plate was allowed to dry for one day and then it was again sprayed with inertol. After a second drying the sand layer is found to adhere strongly enough to the plate so that it is not torn loose by the water streaming through.

The other roughness elements were all soldered onto the plates. For this purpose the plates were first covered over with a thin layer of tin. The spheres, sphere segments and cones, except when they were most closely packed together, were soldered on using sheet aluminum patterns, the short and long angles and the closely packed spheres and spherical segments being soldered on without any pattern. The spheres could be obtained as round shot. Before being soldered on they were given a thin tin coating. The spherical segments were stamped out of galvanized sheet iron 0.3 millimeter thick and the cones were similarly stamped out of thick sheet brass. The angles were formed out of galvanized sheet iron 0.3 millimeter thick. With the exception of the plate having the long angles, the elements were distributed on all the plates as shown in figure 5. The distance between any two elements of the same horizontal row is the same as the distance between two horizontal rows. The rows are staggered as shown in the figure so that each element is centered between the others.

Preliminary Tests

In the preliminary tests there was only the channel shown on figure 4 at the left. The pressure-drop measurements made with the orifices and also with the static tubes, both sides of the wall being smooth, showed a very non-uniform pressure variation along the channel length. It was immediately recognized that the reason for this was the lack of uniformity of the cross sections at the various points of the channel. With the relatively large cross section and therefore small pressure drop, even very small variations in the cross section show greatly disturbing effects on the pressure-drop measurements as may be seen from the following approximate calculation.

TABLE I

Dimensions of the roughness elements k , k' , d , c , D , D/d ; the roughness density F_r/F , F_1/F and the mean channel height b , for the various test plates. For the meaning of d , D , k , k' , c see figure 5. b = mean height of rough channel; F = plate area; F_r = projection of roughness elements on plane normal to direction of flow; F_1 = area of smooth parts of plate between roughness elements.

Type of roughness	Plate No.	d cm	D cm	$\frac{D}{d}$	k cm	c { short angle long angle cm k' cones	b cm	$\frac{F_r}{F}$	$\frac{F_1}{F}$
Spheres	XII	0.41	4	9.75	0.41	-	3.99	0.00785	0.992
Spheres	XIIa	1.0	10	10	1.0	-	-	.00785	.992 ¹
Spheres	III	.41	2	4.88	.41	-	3.99	.0314	.969
Spheres	I	.41	1	2.44	.41	-	3.96	.126	.874
Spheres	II	.41	0.6	1.46	.41	-	3.88	.349	.651
Spheres	V	.41	packed tightly		.41	-	3.68	.907	.093
Spheres	VI	.21	1	4.86	.21	-	3.99	.0314	.969
Spheres	IV	.21	0.5	2.43	.21	-	3.97	.126	.874
Spherical segments	XIII	.8	4	5	.26	-	3.99	.0087	.969
Spherical segments	XIV	.8	3	3.75	.26	-	3.99	.0155	.944
Spherical segments	XV	.8	2	2.5	.26	-	3.98	.0348	.874
Spherical segments	XIX	.8	packed tightly		.26	-	3.85	.251	.093
Cones	XXIII	.8	4	5	.375	0.425	3.99	.0106	.969
Cones	XXIV	.8	3	3.75	.375	.425	3.98	.0189	.944
Cones	XXV	.8	2	2.5	.375	.425	3.95	.0425	.874
Short angles	XVI	-	4	-	.30	.8	4.0	.0151	.998
Short angles	XVIII	-	3	-	.30	.8	4.0	.0269	.996
Short angles	XVII	-	2	-	.30	.8	3.99	.0605	.994
Long angles	XX	-	6	-	.32	17	3.90	.0538	.995
Long angles	XXI	-	4	-	.31	17	3.96	.0776	.992
Long angles	XXII	-	2	-	.30	17	3.96	.152	.985
Hamburg sand	IX	-	-	-	.135	-	3.87	-	-

¹Plate XIIa was measured in large tunnel only.

The mean velocity of the flow is at most $\bar{u} = 8$ meters per second, the hydraulic diameter

$$d_h = \frac{4 \times \text{cross-sectional area}}{\text{wetted perimeter}} = 6.48 \text{ cm}$$

the kinematic viscosity $\nu = 0.012 \text{ cm}^2$ per second, so that the Reynolds Number $Re = \bar{u} \frac{d}{\nu} = 4.3 \times 10^5$. With this Reynolds Number the resistance factor of the smooth pipe is $\lambda = \frac{dp}{dx} \frac{d_h}{q} = 0.018$ where q is the dynamic pressure corresponding to the mean velocity. The frictional pressure drop between two points of measurement at a distance $l = 40 \text{ cm}$ apart is therefore

$$\Delta p = l \frac{dp}{dx} = \lambda \frac{l}{d_h} q = 0.11 q$$

If the channel height b is now assumed to change between the two points by the amount Δb , the width remaining constant, the difference in pressure thus produced is according to the Bernoulli equation

$$\Delta p' = \rho \bar{u} \Delta \bar{u} = \rho \bar{u}^2 \frac{\Delta b}{b} = 2 \frac{\Delta b}{b} q$$

If the error in the pressure drop is not to exceed 2 percent, then

$$\frac{\Delta p'}{\Delta p} < 0.02$$

or

$$2 \frac{\Delta b}{b} < 0.0022, \quad \Delta b < 0.0011 b$$

or finally, with $b = 4 \text{ cm}$

$$\Delta b < 0.0044 \text{ cm} \approx \frac{1}{20} \text{ mm}$$

The channel height must therefore be accurate to $1/20 \text{ mm}$ throughout the channel length if the static pressure measurements are to be considered reliable. It was not possible to attain this accuracy with the channel as first constructed of welded parts and therefore the second channel was made of cast steel as has previously been mentioned and it was then possible by carefully working over the walls to attain the required accuracy.

In the preliminary experiments it was also checked to see whether the flow was uniformly established after reaching the end of the first channel. The starting run is shorter at a rough wall than at a smooth one and it was found that for a small height of roughness the flow could not yet be considered as uniform after the end of its run through the first channel so that after the second cast-steel channel was completed the first was used as an initial runway and this arrangement was kept in the succeeding tests. It was also brought out by the preliminary tests whether in making the pressure drop and velocity-distribution measurements in the second channel, it made any difference whether two smooth walls or one smooth and one rough wall were used. Since this was not the case, two smooth walls were used with the initial run channel for all the main tests.

The pressure drop in the measuring channel proper with both walls smooth was likewise measured in the preliminary tests. A friction factor λ , referred to the hydraulic diameter, was obtained that was found to be in good agreement with the law of resistance of smooth pipes.

It was also investigated by the preliminary tests with a very small channel of rectangular cross section (1.05 x 5 cm) having one rough and one smooth wall whether the velocity profiles at the rough and smooth wall respectively, had any effect on each other. In evaluating the results by the method described in a subsequent section (p. 15), it has been assumed that the friction layers are formed at the smooth and rough wall independently of each other and are the same as for a channel with all smooth or all rough walls. This assumption may be tested in a simple way by plotting the velocity at each wall against the logarithms of the corresponding distances from the walls. Since, according to the generally applicable velocity-distribution law the velocity is proportional to the logarithm of the distance from the wall for both rough and smooth walls the above plot must show a triangular velocity distribution. Figure 7 shows how well it actually does give this distribution.

Before starting the main tests there was also obtained for the outlet section of the measuring channel a diagram showing the lines of equal velocity (fig. 8). The width/depth ratio of 4.25:1 for the rectangle was thus found to be sufficiently large for the flow to be considered as two-dimensional at the center of the section to a sufficient

degree of accuracy, a necessary underlying assumption for the method employed of evaluating the results.

Carrying Out of Main Tests

In the main tests measurements were made to obtain:

1. The velocity profile parallel to the short sides at the center portion of the outlet section.
2. The pressure drop by means of orifices.
3. The temperature.
4. The volume discharged.

In measuring the velocity distribution the total pressure given by the pitot tube was calibrated against the static pressure at the outlet section so that the dynamic pressure was measured directly. In the pressure-drop measurements all possible combinations $p_2 - p_3$, $p_2 - p_4$, ..., $p_2 - p_7$, $p_3 - p_4$, ..., $p_6 - p_7$ were measured so that by taking a mean value it would be possible to balance out small errors occurring in the individual pressure measurements. The pressure at point p_1 was not included since the flow did not assume a steady condition at this point. The arrangement of the roughness elements was such that the last row of elements was directly along the edge of the plate. The pitot tube moved in a plane 1/2 millimeter behind the plate edge. The profile measurements were obtained, as far as possible, at the center of the space between two longitudinal rows of elements. A velocity profile was also measured, however, at the center behind a roughness element. For most of the plates both profiles differed only in the immediate neighborhood of the wall. Only in the case of plate XII (spheres of diameter $d = 4$ mm spaced at distance $D = 40$ mm apart) were any special phenomena observed in connection with the velocity profiles, and these we shall consider later.

In order to keep the motor speed constant the tests were partly conducted using the automatic speed regulator described in the V.D.I., Forschungsheft 356, partly without using it. In the latter case, for the purpose of maintaining uniformity with respect to time of the velocity through the channel between two measuring points, the pressure drop along the channel was controlled by a second

manometer and the throttle of the velocity-measuring apparatus somewhat adjusted.

II. EVALUATION OF TEST RESULTS

Some General Considerations

It is the object of our tests to be able to specify for each type of roughness investigated, a characteristic number by whose aid it becomes possible to predict the resistance for the same type of roughness at other Reynolds Numbers $Re = \bar{u} \frac{d_h}{\nu}$ and relative roughness ratios $\frac{k}{r_h}$ (where r_h is the hydraulic radius) than those directly measured. The number k denotes any useful measure of the absolute roughness and for uniform roughness elements, is most conveniently chosen as the maximum height of the roughness.

Since in the case of sand roughness (grain size denoted by k_s) we possess a type for which the various resistance relations are known over a wide range of Reynolds Numbers and relative roughness, it appeared advantageous to us to evaluate our results in such a manner that they could easily be expressible in terms of the results obtained by Nikuradse for sand roughness without, however, necessarily taking the latter as a standard type of roughness. One objection to using sand roughness as a standard is that this type is not satisfactorily reproducible. If, for example, instead of employing lacquer for gluing the sand to the plates, as was done by Nikuradse, we used some other binding material, and if the time taken for drying was chosen somewhat differently, another sand-grain density and therefore a different resistance, would result.

The above consideration is of little account as far as our method of evaluating the results is concerned, since we consider only the formula giving the resistance factor as a function of the Reynolds Number $Re = \bar{u} \frac{d_h}{\nu}$ and the ratio k_s/r_h but use no comparison values on the roughness densities and absolute roughness. The results of the resistance measurements of Nikuradse are given in figure 1 where λ is shown as a function of $\bar{u}d/\nu$ and k_s/r for a very large range of Reynolds Numbers and relative roughness ratios:

$$10^3 \leq Re \leq 10^6; \quad 507 \geq r/k_s \geq 15$$

The function $\lambda = f(Re, k_s/r)$ assumes a particularly simple form in region I (see Introduction, p. 4) of hydraulically smooth flow, and in region III, of completely rough flow. For region I, λ ceases to depend altogether on k/r and the simple resistance equation (2) for which, in the case of smooth pipes, Nikuradse gives the approximate formula

$$\lambda = 0.0032 + \frac{0.221}{Re^{0.237}} \quad (2a)$$

becomes valid. In region III, the dependence on the relative roughness may be expressed by the simple formula given by von Kármán (reference 3) and by Prandtl and Nikuradse (references 2 and 10), already indicated in the Introduction, namely,

$$\lambda = \left(1.74 + 2 \log \frac{r_h}{k_s}\right)^{-2} \quad (5)$$

the graph of which is shown in figure 9 where r_h denoted the hydraulic radius = $2 \times$ cross section/wetted perimeter.

For the region of transition II, where λ depends on Re as well as on r/k , we have as yet no corresponding analytical formula for λ .

The region of greatest practical importance is by far region III, which extends over a large range of Reynolds Numbers and not too small values of absolute roughness. For this region the relations fortunately assume an exceptionally simple form. According to the measurements of Nikuradse on sand roughness, the purely rough type of flow occurs for the conditions

$$\frac{v_* k_s}{\nu} > 70 \quad \text{or} \quad \frac{\bar{u} d_h}{\nu} > \frac{198}{\sqrt{\lambda}} \frac{d_h}{k_s}$$

In our own series of measurements the relative roughness k/r_h and the Reynolds Numbers were sufficiently large so that the square law of resistance could be held to apply throughout.

Explanation of the Method of Evaluating the Results

Our problem, namely, to specify for each of the types of roughness elements investigated, the resistance of those of similar geometric form but other relative roughness - that is, to extend the results to pipes and channels of other diameters, may be considered as solved if, for each type of roughness we can indicate the value of the "equivalent sand roughness" k_s , that is, the size of sand grain of Nikuradse that has the same resistance as the roughness investigated. No particular physical significance is to be attached to this equivalent roughness but it is rather to be considered as a convenient magnitude that allows us, with the aid of equation (5), to extend the results immediately to the computation of the value of λ for other types of roughness. Instead of k_s we might also use the nondimensional factor

$$\alpha = \frac{k_s}{k}$$

where k denotes the actual absolute roughness (approximately the maximum height of roughness) of the type under consideration.

This process of reducing any arbitrary roughness computation to that of the equivalent sand roughness may be made clearer by an example. We shall take the measurements given by Hopf (reference 7) and Fromm (reference 8) on three different roughnesses, namely, wire netting, "waffle" sheet metal, and saw profile. The measurements were taken for different channel heights, that is, for different relative roughness. For the entirely rough or turbulent type of flow the straight-line equation of slope 2

$$\frac{1}{\sqrt{\lambda}} = a + 2 \log \frac{r}{k} \quad (3)$$

must apply. This equation is found to be fulfilled in a satisfactory manner and the values derived for the constant a are given in table II. By comparison of equation (5) with (3) there is obtained for the reduction coefficient $\alpha = k_s/k$ the relation:

$$2 \log \alpha = 1.74 - a$$

The computed values of α and k_s are likewise given in table II.

TABLE II

Reduction of Measurements of Hopf and Fromm
to Equivalent Sand Roughness

k = absolute roughness; $a = \frac{1}{\sqrt{\lambda}} - 2 \log \frac{r_h}{k}$; k_s = equivalent sand roughness; $\alpha = \frac{k_s}{k}$.

Type of roughness	k cm	a	α	k_s cm
Wire netting	0.0115	0.96	2.46	0.028
Waffle-sheet metal	.0427	1.36	1.52	.065
Saw profile	.15	1.48	1.34	.201

In this manner it is possible to reduce every roughness within the range of the turbulent flow to the equivalent sand roughness if the resistance coefficient is known as a function of the relative roughness.

To determine the equivalent sand roughness k_s it is not necessary, however, to measure every roughness at various relative roughness ratios, a single measurement at one relative roughness only being sufficient as becomes immediately evident from what follows. The amount of testing required is thereby greatly reduced.

In our tests with the rectangular channel having a smooth and rough wall, the determination of k_s is somewhat complicated by the fact that from the pressure-drop measurements we know only the over-all channel resistance which is made up additively of the rough and smooth wall resistances. We therefore still require further information on the resistance of the smooth wall in order to be able to compute the rough wall resistance which alone interests us. The resistance of the smooth wall is obtained, as will be explained directly below, with the aid of the generally applicable velocity-distribution law given above from the measured velocity profile in the vicinity of the smooth wall.

Denoting by τ_r and τ_g the shear stress at the rough and smooth wall, respectively, there is obtained from the equilibrium of shear stresses at the wall with the pressure drop, as a first equation for the determination of the unknowns τ_r and τ_g the relation

$$\tau_r + \tau_g = b \frac{dp}{dx} \quad (6)$$

where b denotes the height of the channel. The velocity distribution law for the friction layer at a smooth and rough wall, respectively, is, according to Prandtl (see Introduction)

$$\frac{u}{v_{*g}} = 5.5 + 5.75 \log \frac{v_{*g} y}{\nu} \quad (\text{smooth wall}) \quad (7)$$

$$\frac{u}{v_{*r}} = A + 5.75 \log \frac{y}{k} \quad (\text{rough wall}) \quad (8)$$

where v_{*g} and v_{*r} denote the "shearing stress velocities" at the rough and smooth wall, respectively, namely,

$$v_{*g} = \sqrt{\frac{\tau_g}{\rho}}, \quad v_{*r} = \sqrt{\frac{\tau_r}{\rho}}$$

and A for the type of roughness in question is a characteristic function which is constant for the region of rough flow but depends on the roughness coefficient v_{*k}/ν in the region of transition from smooth to rough flow. For sand we have for the rough flow, according to the results of Nikuradse, the value of $A_s = 8.48$ and hence the velocity-distribution law for the case of sand roughness becomes

$$\frac{u}{v_{*r}} = 8.48 + 5.75 \log \frac{y}{k_s} \quad (8a)$$

We now make use of the velocity-distribution law for smooth walls (7) to determine the shear stress at the smooth wall from the measured velocity profile. Plotting the measured velocities against the logarithms of the distances from the smooth wall, there is obtained a straight line

$$u = m_g + n_g \log y \quad (7a)$$

whose slope n_g immediately gives τ_g . Comparison of (7) with (7a) gives $n_g = 5.75 v_{*g}$

or

$$v_{*g} = \sqrt{\frac{\tau_g}{\rho}} = \frac{n_g}{5.75} \quad (9)$$

The slope of the profile at the smooth wall can be obtained graphically to a sufficient degree of accuracy. In this method of determining v_{*g} it is assumed that the friction layers at the smooth and rough wall have no mutual effect on each other but that they have the same form as in the symmetrical tunnel. That this is true was shown in the preliminary tests (fig. 7). We may, instead of the shear stresses themselves, use the corresponding velocities v_{*r} and v_{*g} and equation (6) then takes the form

$$v_{*r}^2 + v_{*g}^2 = \frac{b}{\rho} \frac{dp}{dx} \quad (6a)$$

or

$$v_{*r_1} = \sqrt{\frac{b}{\rho} \frac{dp}{dx} - v_{*g}^2} = \sqrt{\frac{b}{\rho} \frac{dp}{dx} - \left(\frac{n_g}{5.75}\right)^2} \quad (10)$$

This is a first method for the determination of the unknown v_{*r} upon which was based the evaluation of our measurements.

Before we proceed to determine from the value of v_{*r} the coefficient $\alpha = \frac{k_s}{k}$ for reducing to equivalent roughness, we shall indicate yet a second and third method for the determination of v_{*r} which are independent of the first one just explained and may therefore be used as a check.

In the same manner that we determined v_{*g} with the aid of the velocity-distribution law for a smooth plate (7), we may use the corresponding law for rough plates (8) to determine v_{*r} . Plotting the measured velocity against the logarithm of the distance $b - y$ from the rough wall we similarly obtain a straight line

$$u = m_r + n_r \log (b - y)$$

from whose slope n_r , by comparison with (8), we find

$$v_{*r_2} = \frac{n_r}{5.75} \quad (11)$$

The slope n_r may also be determined very simply by the graphical method. We have thus determined v_{*r_1} from equation (10) and v_{*r_2} from equation (11) and both values must agree.

It was found that the value of v_{*r_2} generally exceeded somewhat the value of v_{*r_1} (by about 5 percent) and this may be explained as follows. In the measurements of Nikuradse on smooth and rough pipes the result was obtained that the velocity profiles of those portions lying more toward the center of the pipe generally showed a slight systematic deviation from the velocity distribution equations (7) and (8). (See V.D.I., Forschungsheft 356, fig. 24, and V.D.I., Forschungsheft 361, fig. 14.) Most of the measured profiles ran somewhat steeper than the straight line with slope 5.75. In determining v_{*g} and v_{*r} from equations (9) and (11), respectively, we should have taken a somewhat larger value than 5.75, the precise value, however, being unknown. Our obtained values for v_{*g} and v_{*r_2} are therefore consistently somewhat too large, and for this reason v_{*r_1} is found according to (10) to be too small. This explains why v_{*r_2} was generally obtained larger than v_{*r_1} . The actual value of v_{*r} must thus lie between v_{*r_1} and v_{*r_2} and we therefore took the mean of these two values

$$v_{*r} = \frac{1}{2} (v_{*r_1} + v_{*r_2}) \quad (12)$$

as being the nearest approach to the actual value.

Finally, a third method for determining v_{*r} is given by the position of the maximum of the nonsymmetrical velocity profile. If b_1 and b_2 denote the distances, respectively, of this maximum from the smooth and rough wall ($b_1 + b_2 = b$), then, since in completely turbulent flow the shearing stress is a linear function of the distance from the wall and at the maximum velocity $\tau = 0$,

$$\frac{\tau_g}{\tau_r} = \frac{b_1}{b_2}$$

or

$$v_{*r} = \sqrt{\frac{b_2}{b_1}} v_{*g}$$

If v_{*g} has been determined from the velocity-distribution law, then v_{*r} may be computed from the above equation. In evaluating our results we made use of this method for the determination of v_{*r} only as an incidental check.

We now proceed to consider how the results obtained with our types of roughness are reduced to the equivalent sand roughness of Nikuradse. For this purpose we determine, for each type of roughness, the constant A of the universal velocity distribution law.² From equation (8)

$$A = \frac{u}{v_{*r}} - 5.75 \log \frac{y}{k} \quad (13)$$

where k may denote the maximum height of the roughness under consideration. The numerical values of k are given in table I. In equation (13) setting $k = k_s/\alpha$, we find by comparing (13) with (8a) the expression for α :

$$5.75 \log \alpha = 8.48 - A \quad (14)$$

connecting the conversion factor α with the constant A of the velocity-distribution law.

In evaluating our test results we computed, for each velocity profile, a mean value of A from equation (13) using for v_{*r} the mean of the v_{*r_1} and v_{*r_2} values derived above. With the relatively large roughness elements employed the flow obtained was of the purely rough type throughout. This may be seen from the fact that the values of A for each of the profiles differ only slightly from those for a rough plate. (See table III, p. 40.) Out of these values a mean value of A was obtained from all the measurements on one plate (table IV) and with this value of A the coefficient α was determined.

In evaluating the results of the measurements, particular consideration must be given to the measurement of the distance from the rough wall. This distance shall be so defined as to be equal to the distance from a hypothetical smooth wall that replaces the rough wall in such a manner as to keep the fluid volume the same. With both walls smooth the volume of the channel is accurately known (cross section 4.00 by 17.00 cm). Since the volume of the roughness elements may be computed, the mean cross section and therefore the mean channel height with rough and smooth wall is known. These mean channel heights are given in table I for each of the roughness types.

² This is identical with the function $X \frac{v_{*k}}{v}$ employed by Prandtl (reference 2).

Test Results

The results of our tests are summarized in figures 10 to 15 and table III. The measured velocity profiles were evaluated by the method described above. In figures 10 to 15 the results are plotted for each of the types of roughness (spheres, spherical segments, cones, short and long angles) according to the universal velocity-distribution law (u/v_{*r} against $\log y/k$). All profiles measured for the same plate must lie on a single straight line insofar as completely turbulent flow is assumed to hold. The figures show that they actually do so to a sufficient degree of accuracy, each rough plate corresponding to one such straight line and all straight lines running parallel as required by the velocity-distribution law. The slope of these lines is, on the average, somewhat larger than the value 5.75 of the velocity-distribution law. This fact, and the manner in which it has been taken into account, has already been discussed above. That the profiles obtained by us do not coincide with the straight lines of the logarithmic velocity-distribution law so well as those obtained by Nikuradse in his tests on sand roughness is explained by the fact that in our case the ratio of height of roughness to height of channel or pipe radius is considerably larger (approximately $1/8$ as compared to $1/15 - 1/500$). For this reason our profiles, particularly those in the neighborhood of the wall, show greater scattering since here the effect of the individual roughness elements is very prominent. In tables III and IV are given the results of the tests on the rough plates. The former gives for each profile the maximum velocity U , the mean velocity of the profiles at the rough wall \bar{u} , the kinematic viscosity ν , the widths b_1 and b_2 of the smooth and rough profiles, the Reynolds Number $U b/\nu$, the roughness coefficient $v_{*r}k/\nu$, and the roughness function A , and table IV, giving for each of the rough plates the nondimensional shearing stress v_{*r}/\bar{u} , the equivalent sand roughness k_s , the value of $\alpha = k_s/k$, and the mean value of A for each plate. Of the sand-plate tests, only the results obtained with the "Hamburg sand" are given, since the tests with the Gottingen sand are to be considered only as preliminary and carried out with the object of seeing how the results agreed with those obtained by Nikuradse in his tests with sand roughness. The agreement reached between his and our results is satisfactory, the values of λ differing from those found by Nikuradse by 1 to 2 percent.

TABLE IV

$$A = \frac{u}{v_* r} = 5.75 \log \frac{v}{k}, \quad k_s = \text{equivalent sand roughness,}$$

$$\alpha = k_s/k, \quad 5.75 \log \alpha = 8.48 - A$$

Plate No.	$\frac{v_* r}{u}$	A	k_s cm	$\frac{k_s}{k} = \alpha$
Sphere roughness: $k=0.41$ cm				
XII	0.0689	12.2	0.093	0.227
III	.0881	8.92	.344	.838
I	.120	5.68	1.26	3.07
II	.131	5.15	1.56	3.81
V	.0854	9.65	.257	.626
Sphere roughness: $k=0.21$ cm				
VI	0.0779	8.98	0.172	0.819
IV	.106	5.27	.759	3.61
Spherical segment roughness: $k=0.26$ cm				
XIII	0.0590	13.8	0.031	0.118
XIV	.0631	12.7	.049	.186
XV	.0763	9.89	.149	.571
XIX	.0909	7.64	.365	1.40
Cone roughness: $k=0.375$ cm				
XXIII	0.0652	13.1	0.059	0.159
XXIV	.0754	10.6	.164	.437
XXV	.0894	8.49	.374	.996
Short angle roughness: $k=0.30$ cm				
XVI	0.0856	8.56	0.291	0.965
XVIII	.101	6.67	.618	2.05
XVII	.124	4.53	1.47	4.86
Long angle roughness: $k=0.323$ cm, 0.310 cm, 0.303 cm				
XX	0.137	4.17	1.81	5.61
XXI	.167	2.28	3.70	11.9
XXII	.179	2.33	3.56	11.75
Sand roughness: $k=0.135$ cm				
IX	0.0820	7.22	0.222	1.64

The most important, from a practical consideration, of all the magnitudes given in our results is that of k_s , the equivalent sand roughness, which, according to equation (5) and figure 9, makes it possible to apply the results to channels and pipes of other dimensions and also to the towed plate. (See following section.) According to the results obtained for the sand roughness turbulent flow is fully developed for $v_* k_s / \nu > 70$ and the same limit presumably holds for other types of roughness. At any rate our measurements all lie within the range of completely rough or turbulent flow, since according to table III the value of A is practically independent of the Reynolds Number. In applying the results to channels and pipes of other heights and diameters, respectively, it is necessary, however, to consider the limit $v_* k_s / \nu > 70$. In a pipe

$v_* = \frac{\bar{u} \sqrt{\lambda}}{2.83}$ and turbulent flow is obtained when

$$\frac{\bar{u} k_s}{\nu} \sqrt{\lambda} > 198$$

Some exceptional phenomena, the cause of which could not be explained, were observed in obtaining the velocity profiles for plate XII (sphere with $d=4$ mm, $D=40$ mm). To these we shall again refer in section on Velocity Distribution at Plate XII (p. 34). Figure 16 shows a plot of the nondimensional velocity u/v_{*r} against $\log(y/k_s)$ obtained for all the 21 rough plates. The points all fall to a sufficient degree of accuracy on the straight line

$$\frac{u}{v_{*r}} = 8.48 + 5.75 \log \frac{y}{k_s}$$

which was used for the determination of k_s . The scattering is very slight, showing that for all the plates investigated the universal velocity-distribution equation is well satisfied. For only very small values of y/k are there any systematic deviations.

Of particular interest is the dependence of the resistance of rough plates, having equal roughness elements and similar manner of distribution, on the density of the roughness. Figure 17 shows the variation of v_{*r}/\bar{u} with F_r/F for the various plates where F_r denotes the projection of the area of all the roughness elements on a plane normal to the direction of the flow and F is the area of the plate, so that $F_r/F = 0$ denotes a smooth

plate. With increasing F_r/F the resistance at first increases as is to be expected. For the spherical roughness elements, however, the maximum resistance does not occur at the greatest density, but at $F_r/F = 0.4$; that is, when about 40 percent of the total area is covered with spheres. This is also easy to understand since with the elements widely distributed, the entire diameter of the sphere is effective whereas when the packing is closer, only the radius or less becomes the effective absolute roughness. The closest packing of the spherical and spherical segment elements have a lower resistance than that of sand roughness whose grain size is equal to the diameter and height, respectively, of the spheres and spherical segments. For both cases, according to table IV, $k_s/k < 1$. The effective absolute roughness is evidently less for the "regular" roughness due to spheres and spherical segments than for the "irregular" sand roughness.

A maximum is also found for the long angle roughness elements approximately at $F_r/F = 0.1$.

To obtain a still better understanding of the dependence of the resistance on the roughness density, we shall define a resistance coefficient for each type of roughness in the following manner. Let W_r denote the resistance due to the roughness elements alone, that is, the difference between the total resistance W of the rough plate and the resistance W_g of the smooth area between the roughness elements,

$$W_r = W - W_g \quad (15)$$

Further, let u_k denote the velocity at a distance from the wall $y = k$ equal to the height of the roughness. We then form a resistance coefficient

$$C_f = \frac{2W_r}{\rho u_k^2 F_r} \quad (16)$$

where F_r denotes as before the projected area of all the roughness elements on the plane normal to the direction of the flow. (See Sadron, reference 18.) The velocity u_k , when the shear stress at the wall $\tau_r = \rho v_{*r}^2$ is known, may be computed from the velocity-distribution equation (8). With $u = U$ for $y = b_2$, we have from equation (8)

$$\frac{U - u}{v_{*r}} = - 5.75 \log \frac{y}{b_2} = - 2.5 \ln \frac{y}{b_2} \quad (17)$$

and from the above by integration between the limits $y = 0$ and $y = b_2$, we derive the mean velocity \bar{u} of the velocity profile at the rough wall

$$U - \bar{u} = 2.5 v_{*r}$$

Subtracting from the above equation

$$U - u_k = -2.5 v_{*r} \ln \frac{k}{b_2}$$

we obtain

$$u_k - \bar{u} = 2.5 v_{*r} \left(1 + \ln \frac{k}{b_2} \right)$$

or

$$\frac{u_k}{\bar{u}} = 1 - 2.5 \frac{v_{*r}}{\bar{u}} \left(\ln \frac{b_2}{k} - 1 \right) \quad (18)$$

For the resistance W_r , we have from equation (15)

$$W_r = F \rho v_{*r}^2 - F_1 \rho v'_{*g}{}^2$$

or

$$\frac{W_r}{\rho \bar{u}^2} = F \left(\frac{v_{*r}}{\bar{u}} \right)^2 - F_1 \left(\frac{v'_{*g}}{\bar{u}} \right)^2$$

or again

$$C_f = \frac{2W_r}{\rho u_k^2 F_r} = 2 \frac{F}{F_r} \left(\frac{\bar{u}}{u_k} \right)^2 \left[\left(\frac{v_{*r}}{\bar{u}} \right)^2 - \frac{F_1}{F} \left(\frac{v'_{*g}}{\bar{u}} \right)^2 \right] \quad (19)$$

where $\tau' = \rho v'_{*g}{}^2$ denotes the shear stress at the smooth spaces between the roughness elements and F_1 the area of these spaces.

Since \bar{u}/u_k is known from equation (18), we have thus expressed the resistance coefficient C_f in terms of measured magnitudes. The value of v'_{*g}/\bar{u} still depends somewhat on the Reynolds Number, decreasing as the former increases. Since the second term in the brackets is generally small compared to the first, we have replaced, in order to simplify the expression, v'_{*g}/\bar{u} by a mean value which was obtained by measurements on a smooth tinned plate, the value thus found being $\frac{v'_{*g}}{\bar{u}} = 0.0461$. The values of $\frac{u_k}{\bar{u}}$ and the values of C_f computed therefrom by equation (19) are given in table V and plotted in figure

18 as a function of F_r/F . For the spherical segments, cones, and angles, C_f is constant for small values of the roughness density, so that the resistance of the roughness elements depends on the roughness density only through the effect of u_k . At larger values of the roughness densities the C_f curves fall off with increasing F_r/F . The effective height of roughness becomes smaller with the absolute height remaining the same. The C_f curve for the 4.1-millimeter spheres slopes down somewhat even for the smallest measured roughness densities; i.e., in the case of the spherical roughness the processes occurring at each element exert a mutual effect even at smaller roughness densities than those of the other types of roughness elements investigated. The two plates with the 2.1-millimeter spheres fall to some extent on the curve for the 4.1-millimeter spheres, a result that is to be expected from the geometric similarity of the elements.

The three plates with the long angles behave in an exceptional way, the value of C_f first increasing, then decreasing as the roughness density increases. Tests with this type of roughness had previously been carried out by Treer (reference 19), who used values of $F_r/F = 0.5, 0.63, 1.0$, considerably larger than ours. For these large values of roughness densities, he finds an increase in the resistance with increasing roughness density, in agreement with our results.

Finally, we may compare the resistance coefficients C_f of the roughness elements in the boundary layer with the usual resistance coefficients c_w for unconfined flow. For rectangular plates of aspect ratio $l/b = \infty$ and $8/3$ (corresponding to our plates with the long and short angles), set normal to the direction of flow $c_w = 2.01$ and 1.17 , respectively, independent of the Reynolds Number. For spheres at $Re = \bar{u}d/\nu = 2 \times 10^4$ which is about equal to the Reynolds Number of our spherical roughness, $c_w = 0.47$. These values are plotted on figure 18 and it is found that they agree quite well with the C_f values at small roughness densities. It therefore follows that for small roughness densities the resistance of a roughness element in the friction layer is about the same as it would be in an unconfined flow at a velocity of flow equal to that prevailing at the distance from the wall $y = k$ in the friction layer. For our other roughness elements we cannot, unfortunately, make this comparison at present since for these the value of c_w is as yet unknown.

TABLE V

$\frac{F_r}{F}$ = roughness density, C_f = resistance coefficient of roughness element (see equation (19)), u_k = velocity at distance $y = k$ (see equation (18)), $c_{w\infty}$ = resistance coefficient in unconfined flow.

Type of roughness	Plate No.	$\frac{F_r}{F}$	$\frac{\tau_r}{\rho u^2}$	C_f	$\frac{u_k}{\bar{u}}$
Spheres d=0.41 cm	XII	0.00785	0.00474	0.908	0.862
Spheres d=0.41 cm	III	.0314	.00775	.569	.804
Spheres d=0.41 cm	I	.126	.0145	.405	.704
Spheres d=0.41 cm	II	.349	.0172	.195	.678
Spheres d=0.41 cm	V	.907	.00730	.023	.826
Spheres d=0.21 cm	VI	.0314	.00606	.520	.702
Spheres d=0.21 cm	IV	.126	.0112	.498	.570
Spherical segments	XIII	.0087	.00348	.480	.826
Spherical segments	XIV	.0155	.00398	.469	.799
Spherical segments	XV	.0348	.00582	.388	.767
Spherical segments	XIX	.251	.00825	.102	.702
Cones	XXIII	.0106	.00425	.552	.865
Cones	XXIV	.0189	.00569	.561	.832
Cones	XXV	.0425	.00799	.463	.790
Short angles	XVI	.0151	.00732	1.20	.757
Short angles	XVIII	.0269	.0102	1.24	.691
Short angles	XVII	.0605	.0154	1.19	.607
Long angles	XX	.0538	.0188	1.95	.563
Long angles	XXI	.0776	.0279	3.62	.428
Long angles	XXII	.152	.0321	2.54	.378
Sand	IX	-	.00672	-	.594

Sphere, $Re = 2 \times 10^4$: $c_{w\infty} = 0.47$

Rectangular plate, aspect ratio $l/b = 8/3$: $c_{w\infty} = 1.17$

Rectangular plate, aspect ratio $l/b = \infty$: $c_{w\infty} = 2.01$

Extension of Results to Towed Plates

The total resistance of a ship is made up, as is known, of skin-friction resistance, eddy-making resistance, and wave-making resistance - of which the first in many cases forms by far the greatest portion of the total. The frictional resistance depends very strongly on the roughness of the ship's surface. The increase in the resistance due to the surface roughness may amount to 50 percent of the total frictional resistance. The problem of surface roughness is therefore of interest in ship design, particularly as regards the investigation of the resistance offered by rough plates to tangential flow.

Whereas, in the case of pipes and channels, the ratio of the absolute roughness k to the thickness of the friction layer δ is constant all along the pipe, the processes occurring in the friction layer of the towed plate are complicated by the fact that the friction-layer thickness increases from the front toward the rear so that the ratio k/δ on which the resistance depends, decreases from front to rear. After a short initial laminar run the value of k/δ at the forward part of a rough plate is relatively large so that there we have completely turbulent flow. Farther back, provided the plate is long enough and the roughness elements sufficiently small, there is formed the transitional region and beyond this possibly a region of laminar flow.

Prandtl and von Kármán, the former in 1927 and 1932 (references 13 and 14), the latter in 1921 and 1930 (references 12 and 4), have shown for the case of the smooth plate how, from the laws of flow in smooth pipes, there may be derived the law for smooth plates in a purely theoretical way and in good agreement with the results of tests. Using the results of Nikuradse on pipes with sand roughness as a basis, the same method was applied by Prandtl and the author to rough plates (references 15 and 16). These extensions to towed plates were made possible through the discovery of the universal laws for turbulent flow, equations (7) and (8), in smooth and rough pipes. The reliability of this method and its extrapolation beyond the range of tests conducted is assured by the universal character of these laws. For the details of the method the reader is referred to the references cited.

The diagrams obtained in this manner for the local resistance coefficients

$$C_f' = \frac{2\tau}{\rho v^2}$$

and the total resistance coefficients $C_f = \frac{2W}{\rho v^2 b l}$ of the rough plate as a function of the Reynolds Number $R = \frac{v l}{\nu}$ and the relative roughness l/k_s (figs. 19 and 20) have already been given in reference 16 cited above. It is assumed that the flow is turbulent starting from the forward edge. On account of the small region of laminar flow that is always present the total resistance is somewhat lowered, although for relatively long plates this lowering is practically of no importance.

The relations are simplest in the region of completely turbulent flow where the resistance coefficients depend only on the relative roughness. The exact law for the resistance is, however, also in this case, so complicated that it cannot be expressed in explicit form but only as a general function of a parameter (parameter z), namely,

$$l = k_s G(z), \quad W = \rho v^2 b k_s F(z) \quad (20)$$

(b = plate width)

The functions $G(z)$ and $F(z)$ are given in table VI. For practical purposes, however, it is more convenient to possess simple interpolation formulas for the resistance law. For the local and total resistance coefficients C_f' and C_f , we have obtained such formulas as approximate the accurate expression to a sufficient degree of accuracy and are valid for a range $2 \times 10^2 \leq l/k_s \leq 10^6$, namely:

$$\begin{cases} C_f' = \left(2.87 + 1.58 \log \frac{l}{k_s} \right)^{-2.5} \\ C_f = \left(1.89 + 1.62 \log \frac{l}{k_s} \right)^{-2.5} \end{cases} \quad (21a,b)$$

The values of C_f' and C_f are plotted in figure 21 as functions of l/k_s . The corresponding formulas for the smooth plate are

$$\begin{cases} C_f' = (2 \log R - 0.65)^{-2.3} \\ C_f = 0.455 (\log R)^{-2.55} \end{cases} \quad (10^6 \leq R \leq 10^9) \quad (22a,b)$$

Equations (21) are used for the rough plate in place of

equation (5) for the pipe. We are accordingly able, for each type of roughness whose equivalent sand roughness k_s is known, to indicate immediately the local and total resistance coefficients. We shall illustrate by means of an example:

Length of ship $l = 150$ meters, speed of ship $v = 12$ knots per hour = 6.17 meters per second, kinematic viscosity of water at $t = 15^\circ \text{C}$: $\nu = 0.0114$ centimeters per second, Reynolds Number $Re = vl/\nu = 8.12 \times 10^8$. The total resistance coefficient of the smooth ship is, according to (22), $C_f = 1.62 \times 10^{-3}$. We now assume the ship throughout its entire length to possess a roughness of the type of our spherical segments (plate XIII), somewhat corresponding to rivet heads; height $k = 2.6$ millimeters, diameter $d = 8$ millimeters, distance apart $D = 40$ millimeters. The value found for k_s (table V) is $k_s = 0.031$ centimeters. From our equation (21b) with $l/k_s = 4.84 \times 10^5$, we thus compute for the rough surface $C_f = 2.43 \times 10^{-3}$, which is a 50-percent increase as compared with the smooth plate. This is a very large contribution to the resistance but the roughness assumed by us was also considerable.

In order to see to what extent the individual parts of the ship contribute to the total resistance, we shall find the partial resistances W_1 and W_{10} for the first and the tenth parts, respectively, of the ten parts into which the ship's length is assumed to be divided. Denoting by $W = W_1 + W_2 + \dots + W_{10}$ the resistance of the entire ship's surface, we find from our formula (21b)

$$\frac{W_1}{W} = \frac{1}{10} \frac{C_f \left(\frac{l}{10} \right)}{C_f(l)} = 0.149$$

$$\frac{W_{10}}{W} = \frac{C_f(l) - \frac{9}{10} C_f \left(\frac{9}{10} l \right)}{C_f(l)} = 0.081$$

The first tenth portion therefore contributes 14.9 percent and the last tenth only 8.1 percent to the total resistance. From this it may be seen that the same roughness has a considerably more harmful effect at the bow than at the stern.

TABLE VI

Total and local resistance coefficients C_f and C_f' and friction-layer thickness δ/k_s as functions of relative roughness l/k_s in turbulent flow.

l is the length of the plate

k_s , sand roughness

δ , friction-layer thickness

C_f' , local resistance coefficient

C_f , total resistance coefficient

z	$l/k_s = G(z)$	$F(z)$	$C_f' \times 10^3$	$C_f \times 10^3$	δ/k_s
3×10^2	1.615×10^2	1.150	9.84	14.3	1.00×10^1
5×10^2	3.140×10^2	1.832	8.28	11.7	1.67×10^1
7×10^2	4.832×10^2	2.490	7.46	10.3	2.33×10^1
10^3	7.519×10^2	3.453	6.71	9.18	3.33×10^1
2×10^3	1.766×10^3	6.490	5.54	7.35	6.67×10^1
3×10^3	2.878×10^3	9.407	4.99	6.54	1.00×10^2
5×10^3	5.270×10^3	1.503×10^1	4.41	5.70	1.67×10^2
7×10^3	7.841×10^3	2.048×10^1	4.08	5.22	2.33×10^2
10^4	1.195×10^4	2.843×10^1	3.77	4.76	3.33×10^2
2×10^4	2.660×10^4	5.390×10^1	3.26	4.05	6.67×10^2
3×10^4	4.230×10^4	7.845×10^1	3.01	3.71	1.00×10^3
5×10^4	7.564×10^4	1.260×10^2	2.73	3.33	1.67×10^3
7×10^4	1.106×10^5	1.722×10^2	2.57	3.11	2.33×10^3
10^5	1.654×10^5	2.400×10^2	2.41	2.90	3.33×10^3
2×10^5	3.581×10^5	4.581×10^2	2.15	2.56	6.67×10^3
3×10^5	3.611×10^5	6.693×10^2	2.01	2.39	1.00×10^4
5×10^5	9.888×10^5	1.080×10^3	1.86	2.18	1.67×10^4

Formulas (21) are valid only provided the absolute roughness may be considered the same all along the ship's length. The practical problem sometimes arises of finding the resistance of a plate whose roughness varies at different regions. For this case, too, our formulas are still applicable though in passing from one roughness to the other, it is necessary to modify the procedure in the special manner described briefly below.

We shall consider a plate that is of roughness k_{s_1} over a portion of length l_1 and roughness k_{s_2} for the remaining distance l_2 . The resistance of the first portion may be found as usual from formula (21b). In computing the resistance of the remaining portion, however, it is incorrect to take $x = l_1$ as the initial coordinate but another coordinate $x = l_1'$ different from l_1 must be taken. Since in the transition region between the two roughnesses the momentum at the boundary layer varies continuously, l_1' is determined from the condition

$$[W(l_1')]_{k_{s_2}} = [W(l_1)]_{k_{s_1}} \quad (23)$$

i.e., l_1' is that fictitious distance from the leading edge at which, for the roughness k_{s_2} the loss in momentum in the friction layer would be the same as that for roughness k_{s_1} at distance l_1 . To determine l_1' we must use equation (20) from which

$$\frac{l_1}{k_{s_1}} = G(z_1), \quad \frac{l_1'}{k_{s_2}} = G(z_1')$$

The first equation gives the parameter z_1 at the end of the first portion of the plate. The relation between z_1 and z_1' follows from (23), namely,

$$W_1 = \rho v^2 b k_{s_1} F(z_1) = \rho v^2 b k_{s_2} (Fz_1')$$

so that
$$F(z_1') = \frac{k_{s_1}}{k_{s_2}} F(z_1) \quad (24)$$

It is thus possible to compute z_1' from z_1 and therefore also to compute l_1' . The parameter z_2 at the end of the second portion of the plate is then obtained from

$$\frac{l_1' + l_2}{k_{s_2}} = G(z_2)$$

The resistance of the second portion of the plate is

$$W_2 = \rho v^2 b k_{s_2} [F(z_2) - F(z_1')]]$$

so that the resistance of the entire plate is

$$W_1 + W_2 = \rho v^2 b k_{s_2} F(z_2)$$

We shall again illustrate by an example: Let the ship 150 meters long, considered in the previous example, have its roughness for the first 50 meters increased to three times as great as before, $k_s = 0.093$ centimeter, so that

$$l_1 = 50 \text{ m}, \quad k_{s_1} = 0.093 \text{ cm}, \quad l_2 = 100 \text{ m}, \quad k_{s_2} = 0.031 \text{ cm}$$

From $l_1/k_{s_1} = G(z_1) = 5.38 \times 10^4$ there is obtained by (21b):

$$C_f(l_1) = 3.53 \times 10^{-3}$$

From the table for $G(z)$ and $F(z)$, we find by interpolation

$$z_1 = 3.72 \times 10^4: F(z_1) = 95.5$$

and from equation (24), we have:

$$F(z_1') = 286.5, \quad z_1' = 1.22 \times 10^5$$

$$G(z_1') = \frac{l_1'}{k_{s_2}} = 2.06 \times 10^5, \quad l_1' = 63.9 \text{ m}$$

$$\frac{l_1' + l_2}{k_{s_2}} = 5.29 \times 10^5 = G(z_2): z_2 = 2.86 \times 10^5$$

$$F(z_2) = 641, \quad C_f(l_1 + l_2) = 2 \frac{k_{s_2} F(z_2)}{l_1 + l_2} = 2.64 \times 10^{-3}$$

The increase in the resistance due to the greater roughness at the forward third portion of the ship's surface thus amounts to 9 percent.

The computation that was here carried out for a plate with two different roughnesses may of course be easily extended to three or more roughnesses.

We thus possess all the necessary data for computing

the required resistance for any rough surface of a ship whose "equivalent sand roughness" k_s has been obtained by experiment in our channel.

Our test apparatus, which may now be considered as having attained its final form, makes it possible to investigate every type of roughness that may occur in practice, particularly the surface roughness of ships. It is only necessary by the above process to determine in each case the roughness function $A = A \left(\frac{v_* k}{v} \right)$. In the turbulent region, where A is constant and independent of $\frac{v_* k}{v}$ it is possible, with the aid of the equivalent sand roughness k_s , according to formulas (5) and (21a,b), to extend the computations to other pipes and channels as well as to towed plates. In this way the plate towing tests for the determination of the ship's resistance, which are often very difficult to carry out, are replaced by the much simpler tests in our channel.

For the region of transition where the roughness function A depends on $\frac{v_* k}{v}$, the extension of the results to other pipes and channels and to towed plates is possible only if the roughness function $A = A \left(\frac{v_* k}{v} \right)$ is accurately known. This function probably depends also on the quality of the roughness, and further investigation is necessary.

Velocity Distribution at Plate XII

In measuring the velocity field in the neighborhood of the rough wall of plate XII (diameter of sphere = 4 mm, separating distance = 40 mm (see fig. 6a)), a peculiar phenomenon was observed which appears to be so contrary to all our present-day views on turbulent velocity distribution that it seems worth while to describe it here briefly.

In figures 22 and 23 are shown the velocity distribution diagrams for two planes normal to the rough plate, the lines connecting points of equal velocity. Figure 22 is for the plane immediately behind the last row of spheres while figure 23 is for a plane 40 millimeters behind this row. In the former the sphere a lying directly in front of the pitot tube naturally causes large velocity losses. From an examination of both of the figures, however, it is clear that the smallest velocities occur at the free spaces

between the spheres and the greatest velocities occur behind the rows of spheres where a greater reduction in velocity should be expected. In figure 23, for example, the spheres b and c, 4 centimeters from the measuring plane, and sphere e, 8 centimeters away, clearly show excess velocities and the same is true for spheres b and c in figure 22. The shielding effect of the rows of spheres is therefore, so to speak, negative. This phenomenon was observed for this one plate alone having the maximum sphere separation. The phenomenon clearly shows that the disturbance produced by the individual spheres is so strong that it reaches over to the neighboring spheres, so that the processes at each of the spheres have an effect on each other even at the relatively great distance of separation with $D/d = 10$. The effect also expressed itself in the value of the resistance coefficients C_f for the individual roughness elements (fig. 18).

In order to check whether this phenomenon was not due to the limited cross-sectional area of the channel flow and possibly caused by the interference effect of the oppositely lying wall, the same roughness was enlarged so as to be geometrically similar (sphere diameter = 10 mm, distance apart = 100 mm) and the plate, 150 centimeters long, was investigated in the large Gottingen wind tunnel (jet diameter = 2.25 meters). Exactly the same phenomenon was again observed, showing that it was not brought about by the fact that the stream was restricted to a finite cross section but that it was a pure friction-layer phenomenon. No satisfactory explanation of this phenomenon has as yet been found. Possibly complicated secondary flows have something to do with it. At any rate, it appears that the turbulent mixing processes behind obstacles in the neighborhood of walls are in some respects very different from those behind obstacles in an unconfined flow.

SUMMARY

Based on the universal laws of turbulent velocity distribution at rough and smooth walls, there is in the present work presented a method that allows surface roughness tests and in particular, measurements on the roughness of ship surfaces to be carried out in a much simpler manner than was done heretofore. The types of roughness investigated were in the form of flat, rough plates installed in a square-section rectangular channel, the other three walls

always being smooth. Twenty-one plates of various roughness were investigated, the roughness elements being the following: spheres of diameter 0.41 and 0.21, respectively, spherical segments, cones, and "short" and "long" angles. The absolute roughness or roughness height k was 2 to 4 centimeters. The pattern, according to which the elements were distributed, was the same for each plate while the density of the roughness was varied.

For each rough plate the nonsymmetrical velocity distribution was measured for six different velocities at the outlet section of the channel and the pressure drop obtained by orifices in the rough wall. Preliminary tests established the fact that the velocity profiles at the smooth and rough walls exerted no interference effect on each other, each velocity distribution being the same as if the walls were all smooth or all rough, respectively. From the measured nonsymmetrical velocity distribution, it is therefore possible with the aid of the velocity-distribution law, to determine the shear stress τ_g at the smooth wall and the required shear stress at the rough wall τ_r is then found from the equation

$$\tau_r + \tau_g = \frac{b}{\rho} \frac{dp}{dx}$$

where b is the channel height. For almost all the roughnesses and velocities investigated, the resistance was independent of the Reynolds Number. In order to apply the results of the measurements conveniently to channels and pipes of other hydraulic radii r_h and to towed plates, there was determined for each of the roughnesses investigated an "equivalent sand roughness" k_s which is the grain size of the sand roughness as used in the tests of Nikuradse, and has the same resistance as the corresponding roughness elements.

Besides depending on the relative roughness r_h/k , the resistance also depends on a second roughness parameter, namely, the roughness density F_r/F where F_r is the total projected area of the roughness elements on a plane normal to the direction of flow and F is the plate area. In determining the dependence of the resistance on the roughness density F_r/F the fact was established that the maximum resistance does not occur at the maximum roughness density but at a considerably lower value. Furthermore, for each of the rough plates was determined the coefficient C_f of the roughness element referred to the

velocity u_k at distance $y = k$ and defined by the equation

$$C_f = \frac{2W_r}{\rho u_k^2 F_r}$$

where W_r denoted the resistance of the rough portion of the surface (after subtracting that of the smooth areas between the roughness elements). It was found that for nearly all the types of roughness elements the value of C_f is independent of the roughness density F_r/F for small values of the former and falls off sharply for large values. The resistance coefficient C_f of the individual roughness elements practically agrees in value with the coefficient in an unconfined stream for the same Reynolds Number.

For each of the elements whose equivalent roughness k_s was determined in the manner indicated, the results could be extended immediately to find the resistance of the towed plate with the aid of a diagram given by L. Prandtl and H. Schlichting in a previous work on the resistance of rough plates. For the region in which the turbulent flow-resistance law applies, simple interpolation formulas are given for the local and total resistance coefficients of the towed plate.

Translation by S. Reiss,
National Advisory Committee
for Aeronautics.

REFERENCES

1. Prandtl, L.: Über die ausgebildete Turbulenz. Verh. 2. internat. Kongr. techn. Mech., S. 62. Zurich, 1927.
2. Prandtl, L.: Recent Results of Turbulence Research. T.M. No. 720, N.A.C.A., 1933.
3. von Kármán, Th.: Mechanische Ähnlichkeit und Turbulenz. Verh. d. 3. internat. Kongr. techn. Mech. Stockholm, 1930.
4. von Kármán, Th.: Nachr. Ged. Wiss., Göttingen, Math.-phys. Klasse, 1930, S. 58.
5. Nikuradse, J.: Untersuchungen über die Geschwindigkeitsverteilung in turbulenten Strömungen. Forsch.-Arb. Ing.-Wes., Heft 281. Berlin, 1926.
6. Nikuradse, J.: Gesetzmässigkeiten der turbulenten Strömung in glatten Röhren. Forsch.-Arb. Ing.-Wes., Heft 356. Berlin, 1932.
7. Hopf, L.: Z.f.a.M.M. 3 (1923), S. 329.
8. Fromm, K.: Z.f.a.M.M. 3 (1923), S. 339.
9. Fritsch, W.: Z.f.a.M.M. 8 (1928), S. 199.
10. Nikuradse, J.: Strömungsgesetze in rauhen Röhren. Forsch.-Arb. Ing.-Wes., Heft 361. Berlin, 1933.
11. Kempf, G.: Weitere Reibungsergebnisse an ebenen glatten und rauhen Flächen. Hydromechanische Probleme des Schiffsantriebs. Hamburg, 1932, S. 87.
12. von Kármán, Th.: Z.f.a.M.M. 1 (1921), S. 233.
13. Prandtl, L.: Über den Reibungswiderstand strömender Luft. Ergb. Aero. Vers. Göttingen, III. Lief. (1927), S. 1.
14. Prandtl, L.: Zur turbulenten Strömung in Röhren und langs Platten. Ergb. Aero. Vers. Göttingen, IV Lief. (1932), S. 18.

REFERENCES (Cont.)

15. Prandtl, L.: Reibungswiderstand. Hydromechanische Probleme des Schiffsantriebs. Hamburg, 1932, S. 87.
16. Prandtl, L., and Schlichting, H.: Werft-Reederei Hafen, 1934, S. 1.
17. Kempf, G.: Werft-Reederei Hafen, 1929, S. 234 u. 247.
18. Sadron, Ch.: C. R. Acad. Sci. Paris 200 (1935), S. 292.
19. Treer, M. F.: Physik. Z. XXX (1929), S. 539.
20. Prandtl, L.: Abriss der Strömungslehre, Braunschweig, 1931, S. 139.

TABLE III

U = maximum velocity, \bar{u} = mean velocity of the profile at the rough wall, $\frac{1}{\rho} \frac{dp}{dx}$ = pressure drop, ν = kinematic viscosity, ρ = density, b_1 = distance of maximum velocity from smooth wall, b_2 = distance of maximum velocity from rough wall, $v_{*g} = \sqrt{\frac{\tau_g}{\rho}}$ = "shear stress velocity" at smooth wall, $v_{*r} = \sqrt{\frac{\tau_r}{\rho}}$ = shear stress velocity at rough wall, τ_g = shear stress at smooth wall, τ_r = shear stress at rough wall, $Re = \frac{U b}{\nu}$ = Reynolds Number, $\frac{v_{*r} k}{\nu}$ = roughness coefficient.

Plate No.	Profile No.	U cm/sec	\bar{u} cm/sec	$\frac{1}{\rho} \frac{dp}{dx}$ cm/sec ²	ν cm ² /sec	b_1 cm	b_2 cm	v_{*r} cm/sec	v_{*g} cm/sec	$\frac{v_{*r}}{\nu}$	$\frac{U b}{\nu} \cdot 10^{-3}$	$\frac{v_{*r} k}{\nu} \cdot 10^{-2}$	A
Sphere roughness: $k = 0.41$ cm													
XII	1	321	280	148	0.0117	1.51	2.48	19.4	14.1	0.073	109	6.80	12.16
	2	385	339	204	0.0116	1.49	2.50	23.3	16.2	0.069	132	8.24	12.21
	3	476	419	302	0.0116	1.49	2.50	28.8	18.8	0.069	164	10.2	12.19
	4	547	480	393	0.0115	1.52	2.47	33.1	21.7	0.068	190	11.8	12.22
	5	650	569	546	0.0115	1.52	2.47	39.4	27.0	0.067	224	14.0	12.14
III	1	316	270	185	0.0117	1.06	2.93	23.5	15.1	0.086	108	8.34	8.91
	2	391	333	274	0.0113	1.16	2.83	29.1	17.1	0.086	122	10.5	8.95
	3	500	424	441	0.0114	1.27	2.72	37.2	22.4	0.087	175	13.4	8.94
	4	568	481	566	0.0112	1.26	2.73	42.2	24.5	0.088	202	15.5	8.93
	5	704	588	856	0.0113	1.42	2.57	52.3	29.9	0.090	249	19.0	8.93
	6	816	686	1145	0.0114	1.26	2.73	60.4	34.3	0.085	285	21.7	8.91
I	1	310	248	278	0.0115	0.91	3.05	29.6	13.1	0.124	107	10.6	5.68
	2	384	306	412	0.0116	0.96	3.00	36.6	15.3	0.122	131	12.95	5.69
	3	508	403	708	0.0120	1.01	2.95	48.5	22.6	0.120	168	16.6	5.66
	4	566	450	870	0.0116	1.01	2.95	54.0	25.4	0.118	218	19.1	5.68
	5	658	523	1165	0.0116	0.96	3.00	62.8	28.0	0.119	225	22.2	5.68
	6	778	626	1622	0.0118	0.96	3.00	74.2	33.1	0.116	261	25.9	5.70
II	1	313	240	260	0.0114	0.98	2.90	31.4	13.7	0.130	107	11.3	5.20
	2	384	297	403	0.0115	0.90	2.98	38.7	15.7	0.129	130	13.8	5.18
	3	500	384	696	0.0116	0.90	2.98	50.2	20.2	0.132	167	17.8	5.13
	4	568	438	908	0.0117	0.88	3.00	57.0	23.7	0.131	187	20.0	5.14
	5	646	499	1184	0.0113	0.90	2.98	65.0	26.3	0.128	222	23.6	5.14
	6	746	572	1585	0.0112	0.92	2.96	75.0	29.2	0.128	258	27.5	5.11
V	1	311	259	186	0.0116	1.16	2.52	22.2	14.8	0.087	86	7.85	9.61
	2	385	322	284	0.0115	1.16	2.52	27.5	17.7	0.085	123	9.81	9.69
	3	498	417	473	0.0114	1.16	2.52	35.6	22.9	0.084	161	12.8	9.64
	4	585	489	648	0.0113	1.16	2.52	41.8	26.2	0.086	190	15.2	9.64
	5	662	554	833	0.0114	1.16	2.52	47.3	29.8	0.085	214	17.0	9.67
	6	809	678	1247	0.0113	1.16	2.52	57.8	35.5	0.085	263	21.0	9.63

Continued on following pages.

Table III (cont.)

Plate No.	Profile No.	U cm/sec	u cm/sec	$\frac{1}{\rho} \frac{dp}{dx}$ cm/sec ²	ν cm ² /sec	b_1 cm	b_2 cm	$v_{s,r}$ cm/sec	$v_{s,t}$ cm/sec	$\frac{v_{s,r}}{u}$	$\frac{U b_1 \cdot 10^{-3}}{\nu}$	$\frac{v_{s,r} k}{\nu} \cdot 10^{-2}$	A
Sphere roughness: $d = k = 0,21$ cm													
VI	1	316	269	154	0,0116	1,36	2,63	20,8	13,9	0,077	109	3,76	8,96
	2	390	333	234	0,0116	1,36	2,63	25,7	17,6	0,075	134	4,65	9,02
	3	491	419	365	0,0116	1,35	2,64	32,4	20,2	0,077	169	5,86	8,99
	4	566	481	480	0,0114	1,35	2,64	37,3	22,8	0,078	198	6,87	8,97
	5	664	567	656	0,0114	1,35	2,64	43,8	27,7	0,078	232	8,07	8,99
	6	806	660	966	0,0118	1,35	2,64	53,2	33,2	0,082	273	9,46	8,95
IV	1	325	261	242	0,0120	1,06	2,91	27,7	13,6	0,108	108	4,85	5,24
	2	396	319	348	0,0121	1,07	2,90	33,8	18,1	0,105	130	5,87	5,31
	3	572	459	704	0,0122	1,11	2,86	48,8	22,6	0,107	186	8,40	5,32
	4	646	514	888	0,0125	1,11	2,86	55,1	25,9	0,107	205	9,26	5,25
	5	751	606	1196	0,0121	1,01	2,96	64,1	30,1	0,105	246	11,1	5,24
Spherical segment roughness: $k = 0,26$ cm													
XIII	1	314	279	124	0,0110	1,61	2,38	16,4	14,5	0,061	114	3,89	13,80
	2	389	345	177	0,0110	1,66	2,33	20,3	17,8	0,059	141	4,82	13,85
	3	495	438	278	0,0112	1,76	2,23	25,9	20,7	0,060	176	6,02	13,86
	4	574	508	367	0,0112	1,62	2,37	30,0	23,5	0,060	220	6,98	13,78
	5	648	573	462	0,0112	1,63	2,36	33,8	28,2	0,058	231	7,88	13,77
	6	830	735	750	0,0110	1,79	2,20	43,3	37,1	0,057	301	10,3	13,91
XIV	1	380	334	181	0,0113	1,56	2,43	20,9	17,8	0,063	134	4,83	12,76
	2	497	431	298	0,0114	1,62	2,37	27,3	21,6	0,065	174	6,26	12,62
	3	572	498	390	0,0116	1,62	2,37	31,5	23,8	0,064	197	7,08	12,67
	4	700	609	570	0,0114	1,57	2,42	38,5	32,0	0,062	246	8,82	12,70
	5	834	730	800	0,0114	1,62	2,37	45,9	38,4	0,059	292	10,5	12,75
XV	1	382	328	223	0,0113	1,54	2,44	25,0	16,5	0,078	135	5,77	9,85
	2	502	428	375	0,0118	1,52	2,46	32,8	20,4	0,078	169	7,58	9,77
	3	564	483	472	0,0118	1,58	2,40	36,9	23,8	0,075	190	8,16	9,86
	4	687	592	695	0,0117	1,62	2,36	45,0	30,3	0,073	244	10,0	9,94
	5	817	710	977	0,0114	1,61	2,37	53,4	34,8	0,074	284	12,3	10,04
XIX	1	316	264	198	0,0114	1,17	2,68	23,8	14,1	0,091	105	5,46	7,68
	2	386	319	294	0,0113	1,27	2,58	29,2	17,4	0,091	132	6,74	7,66
	3	480	401	452	0,0116	1,17	2,68	36,2	20,4	0,090	159	8,16	7,66
	4	563	471	620	0,0117	1,17	2,68	42,5	26,6	0,088	184	9,49	7,66
	5	671	553	880	0,0115	1,25	2,60	50,6	28,5	0,093	224	11,5	7,62
	6	818	673	1305	0,0112	1,27	2,58	61,8	34,5	0,092	281	14,4	7,58
Cone roughness: $k = 0,375$ cm													
XXIII	1	321	281	130	0,0110	1,56	2,43	18,2	14,4	0,064	116	6,21	13,07
	2	386	335	185	0,0109	1,70	2,29	21,9	16,7	0,066	141	7,54	13,08
	3	488	427	291	0,0109	1,64	2,35	27,7	21,2	0,064	178	9,54	13,10
	4	574	497	403	0,0108	1,72	2,27	32,6	24,6	0,067	212	11,3	13,04
	5	668	578	542	0,0106	1,74	2,25	38,0	27,6	0,067	252	13,4	13,08
XXIV	1	307	260	147	0,0108	1,49	2,49	20,1	13,4	0,081	113	6,99	10,52
	2	384	326	218	0,0108	1,49	2,49	25,2	16,4	0,081	143	8,74	10,50
	3	495	423	350	0,0107	1,48	2,50	32,5	20,5	0,077	184	11,4	10,59
	4	567	485	452	0,0108	1,49	2,49	37,2	24,0	0,075	207	12,9	10,59
	5	662	564	605	0,0106	1,52	2,46	43,4	28,0	0,074	248	15,4	10,56
	6	890	756	1076	0,0109	1,50	2,48	58,4	36,2	0,076	325	20,1	10,54

Table III (cont.)

Plate No.	Profile No.	U cm/sec	\bar{u} cm/sec	$\frac{Idp}{\rho dx}$ cm/sec ²	ν cm ² /sec	b_1 cm	b_2 cm	$v_{.r}$ cm/sec	$v_{.s}$ cm/sec	$\frac{v_{.r}}{u}$	$\frac{U b}{\nu} \cdot 10^{-3}$	$\frac{v_{.r} k}{\nu} \cdot 10^{-2}$	β
XXV	1	310	257	176	0,0107	1,33	2,62	23,4	12,2	0,096	115	8,19	8,41
	2	388	324	267	0,0107	1,32	2,63	29,2	16,9	0,090	144	10,3	8,48
	3	476	397	401	0,0106	1,36	2,59	35,9	20,7	0,089	172	12,7	8,51
	4	564	470	562	0,0107	1,35	2,60	42,5	23,3	0,091	208	14,9	8,50
	5	668	555	788	0,0106	1,42	2,53	50,4	27,7	0,089	249	17,8	8,54
	6	787	660	1086	0,0105	1,30	2,65	59,3	32,0	0,089	296	21,2	8,54
"Short angle" roughness: $k = 0,30$ cm													
XVI	1	318	267	175	0,0112	1,52	2,48	23,1	12,5	0,089	113	6,24	8,54
	2	389	328	254	0,0112	1,46	2,54	28,2	15,5	0,088	139	7,62	8,52
	3	497	422	415	0,0110	1,40	2,60	36,1	19,3	0,086	181	9,91	8,54
	4	566	482	534	0,0110	1,40	2,60	41,1	23,0	0,083	206	11,3	8,58
	5	666	563	737	0,0111	1,46	2,54	48,4	27,5	0,085	240	13,2	8,57
	6	789	671	1030	0,0108	1,46	2,54	57,2	32,9	0,084	259	16,0	8,64
XVIII	1	380	310	300	0,0114	1,24	2,76	31,6	14,6	0,102	133	8,38	6,62
	2	498	411	514	0,0117	1,21	2,79	41,4	18,4	0,100	170	10,7	6,66
	3	562	463	654	0,0116	1,21	2,79	46,8	20,0	0,102	194	12,2	6,66
	4	666	547	921	0,0116	1,21	2,79	55,4	23,8	0,102	230	14,4	6,66
	5	796	661	1310	0,0114	1,22	2,78	66,2	31,3	0,100	279	17,5	6,76
XVII	1	313	239	301	0,0111	1,07	2,92	31,6	13,1	0,138	113	8,60	4,39
	2	385	296	440	0,0113	1,07	2,92	38,9	16,0	0,138	136	10,4	4,43
	3	501	400	722	0,0116	1,11	2,88	50,6	18,4	0,123	172	13,2	4,63
	4	567	451	925	0,0116	1,11	2,88	57,3	21,6	0,124	195	14,9	4,62
	5	674	527	1292	0,0111	1,11	2,88	68,1	28,4	0,127	242	18,5	4,53
	6	773	616	1693	0,0113	1,01	2,98	78,1	31,2	0,124	272	20,9	4,59
"Long angle" roughness: $k = 0,32$ cm													
XX	1	316	240	334	0,0116	0,72	3,18	32,9	10,8	0,134	106	9,16	4,20
	2	388	291	500	0,0117	0,80	3,10	40,4	12,2	0,140	126	11,1	4,19
	3	515	399	865	0,0120	0,72	3,18	53,6	13,9	0,133	167	14,4	4,19
	4	578	445	1092	0,0120	0,74	3,16	60,2	20,1	0,135	188	16,2	4,18
	5	658	498	1408	0,0117	0,75	3,15	68,5	21,6	0,142	220	18,9	4,12
$k = 0,31$ cm													
XXI	1	313	214	450	0,0117	0,66	3,30	38,8	11,3	0,192	106	10,3	2,22
	2	388	270	648	0,0117	0,62	3,34	48,1	13,3	0,182	131	12,7	2,25
	3	488	348	975	0,0117	0,58	3,38	60,6	15,6	0,172	165	16,1	2,29
	4	566	413	1281	0,0116	0,63	3,33	70,3	17,9	0,167	193	18,8	2,30
	5	722	529	2022	0,0114	0,68	3,28	89,7	28,4	0,162	250	24,4	2,36
$k = 0,30$ cm													
XXII	1	315	214	392	0,0109	0,69	3,27	38,7	9,8	0,182	115	10,8	2,30
	2	394	270	605	0,0108	0,67	3,29	48,4	12,3	0,180	145	13,6	2,33
	3	484	339	920	0,0112	0,59	3,37	59,0	14,4	0,171	171	16,0	2,41
	4	567	389	1270	0,0112	0,65	3,31	69,6	16,1	0,179	200	18,8	2,32
	5	666	456	1740	0,0108	0,64	3,32	81,8	19,7	0,180	244	22,9	2,30
	6	749	512	2200	0,0110	0,64	3,32	92,0	24,0	0,180	270	25,3	2,31
Roughness, Hamburg sand: $k = 0,135$ cm													
IX	1	319	270	181	0,0116	1,25	2,62	22,0	14,5	0,083	106	2,56	7,27
	2	420	354	297	0,0118	1,22	2,65	29,0	19,1	0,081	138	3,32	7,19
	3	501	423	416	0,0120	1,19	2,68	34,6	21,9	0,080	162	3,89	7,20
	4	564	472	516	0,0116	1,28	2,59	38,9	23,3	0,083	188	4,53	7,46
	5	654	546	692	0,0119	1,18	2,69	45,1	28,1	0,082	212	5,12	7,11
	6	763	639	933	0,0121	1,16	2,71	52,6	31,3	0,082	244	5,86	7,11

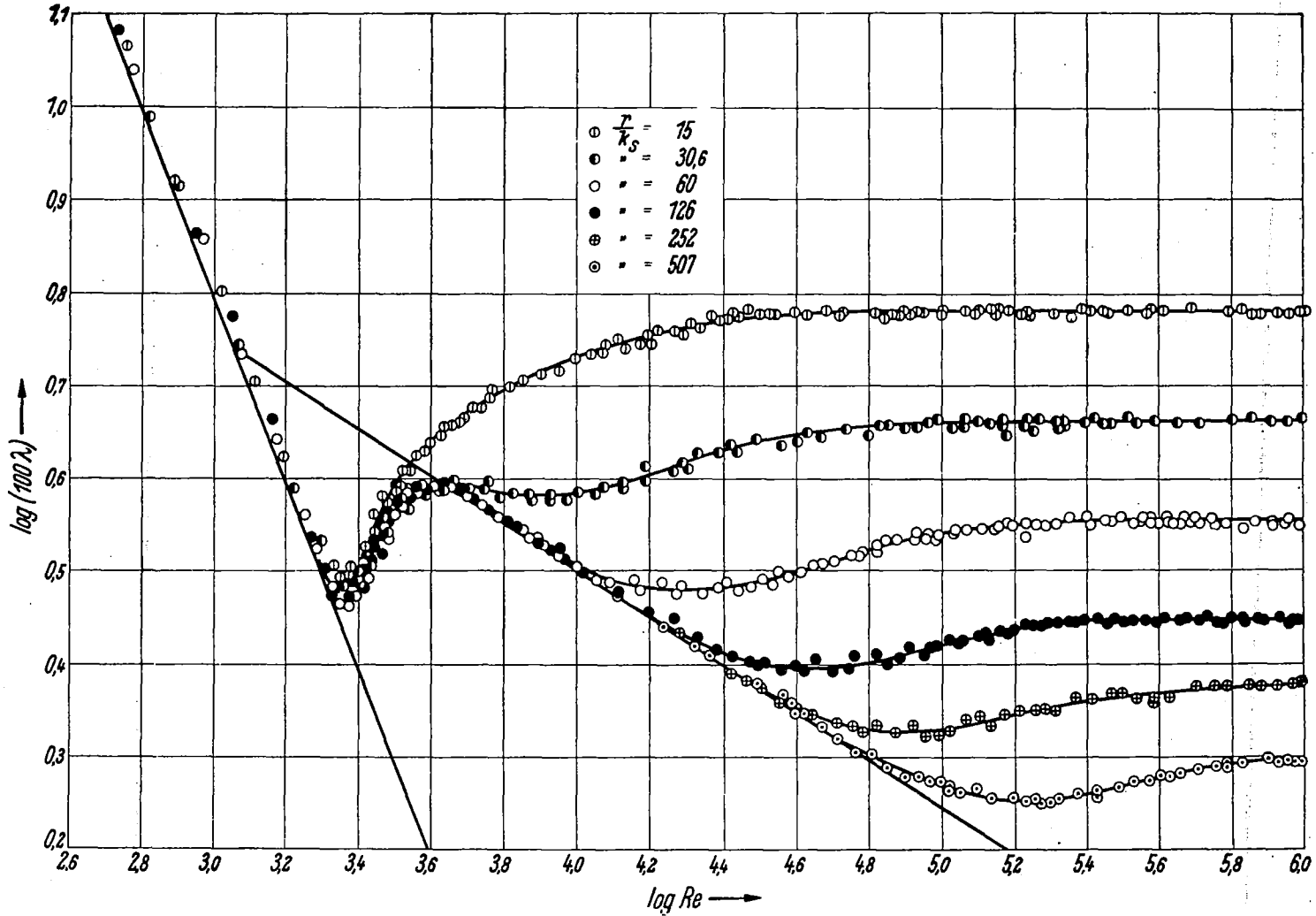


Figure 1.- The resistance factor $\lambda = \frac{dp}{dx} \frac{2d}{\rho \bar{u}^2}$ of rough pipes as a function of the Reynolds Number $Re = \frac{\bar{u}d}{\nu}$ and the relative roughness r/k_s for sand roughness (after Nikuradse).

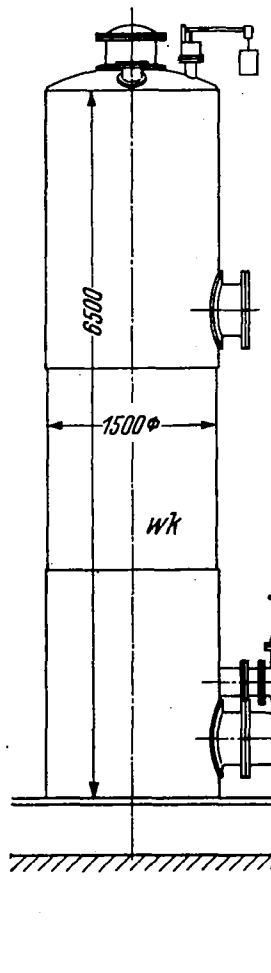


Figure 2.- Test set-up for the roughness measurements.
 wk=water tank; zr=inlet pipe; ak=channel for initial run; mk=measuring channel; gm=velocity measuring apparatus; kp=centrifugal pump; vk=storage channel; mb=measuring tank; fl=pulley; sb₁=valve between pump and tank; sb₂=valve between tank and inlet pipe.

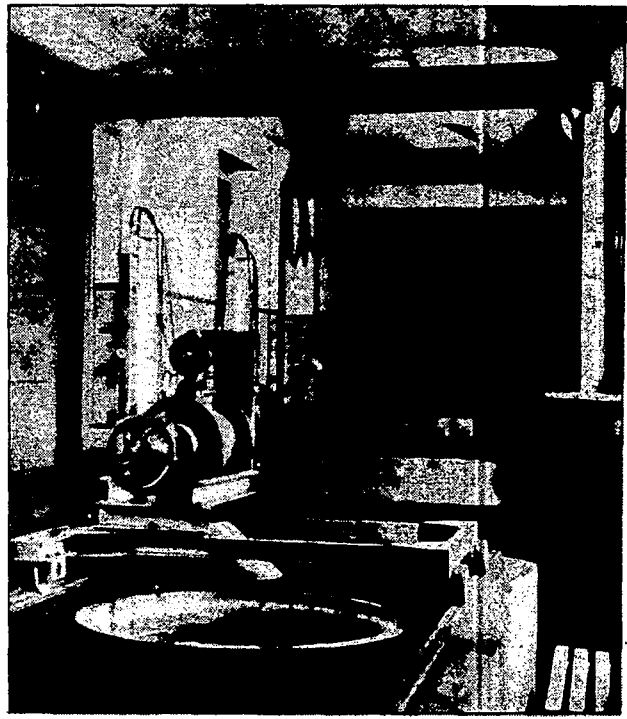
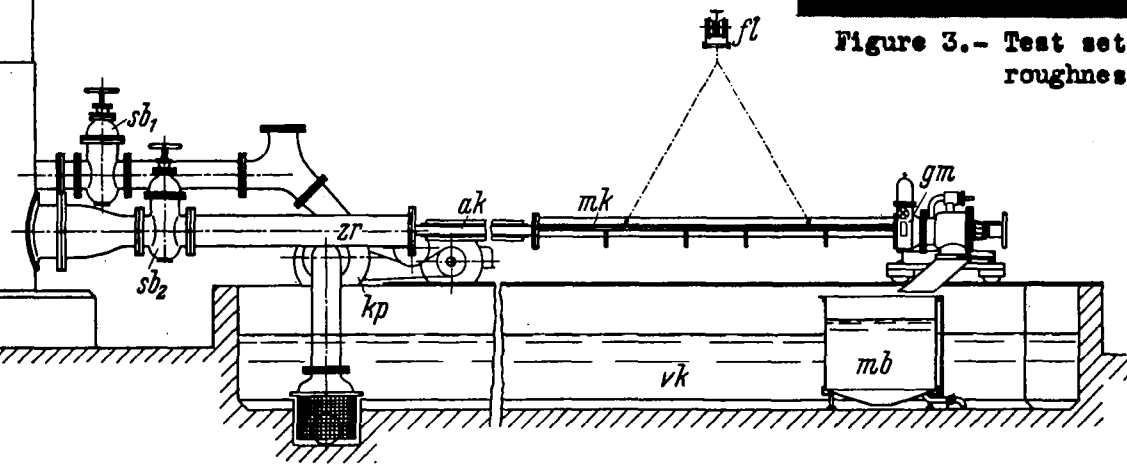


Figure 3.- Test set-up for surface roughness measurements.

Figure 4.- Test channel for surface roughness measurement.

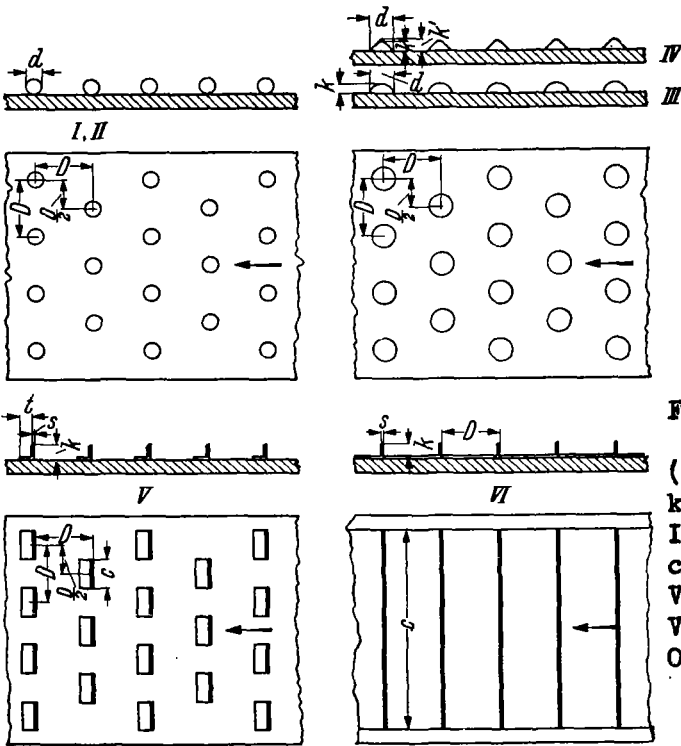
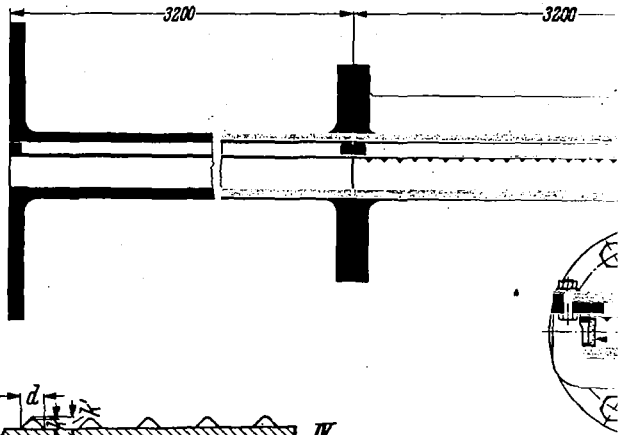


Figure 5.- Dimensional distribution of roughness (see Table I). I, $k=0.41$ and 0.21 cm; III=spherical segments, $k=0.41$ and 0.21 cm.; IV=cones, $k=0.41$ and 0.21 cm.; V=short angles, $k=0.41$ and 0.21 cm.; VI=long angles, $k=0.41$ and 0.21 cm.

- $u=400$ cm/sec
- $u=475$ cm/sec
- $u=525$ cm/sec
- $u=560$ cm/sec
- $u=450$ "
- $u=500$ "
- $u=550$ "

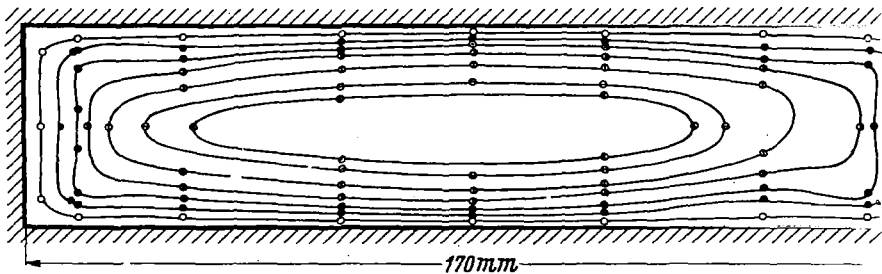


Figure 8.- Lines of equal velocity at outlet section of channel obtained with both walls smooth.



Figure 6a- Spheres, Plate XII.

$d = 0.41$ cm; $k = 0.41$ cm;
 $D = 4.0$ cm; $k_s = 0.093$ cm.

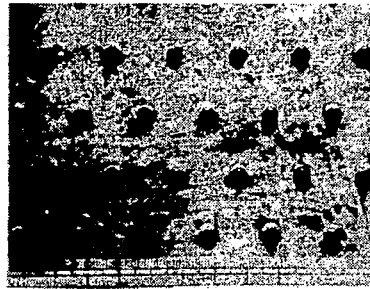


Figure 6b- Spheres, Plate III.

$d = 0.41$ cm; $k = 0.41$ cm;
 $D = 2.0$ cm; $k_s = 0.344$ cm.

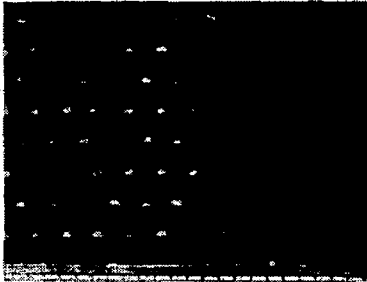


Fig. 6c- Spheres, Plate I.

$d = 0.41$ cm; $k = 0.41$ cm;
 $D = 1.0$ cm; $k_s = 1.26$ cm.

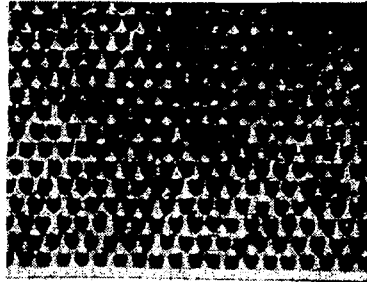


Fig. 6d- Spheres, Plate II.

$d = 0.41$ cm; $k = 0.41$ cm;
 $D = 0.6$ cm; $k_s = 1.56$ cm.

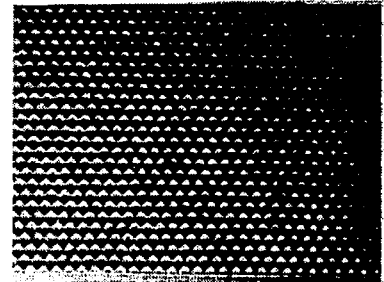


Fig. 6e- Spheres, Plate V.

$d = 0.41$ cm; $k = 0.41$ cm;
 dichteste Packung; $k_s = 0.257$ cm.

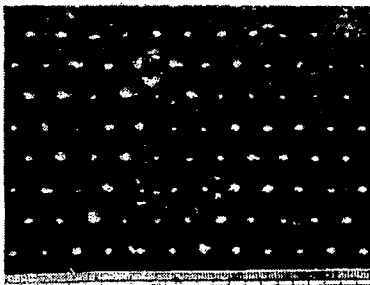


Figure 6f- Spheres, Plate VI.

$d = 0.21$ cm; $k = 0.21$ cm;
 $D = 1.0$ cm; $k_s = 0.172$ cm.

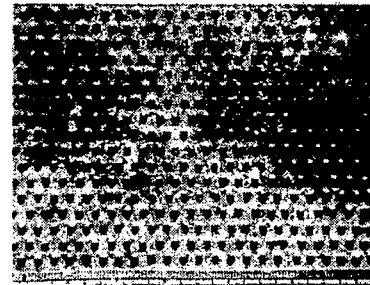


Figure 6g- Spheres, Plate IV.

$d = 0.21$ cm; $k = 0.21$ cm;
 $D = 0.5$ cm; $k_s = 0.759$ cm.

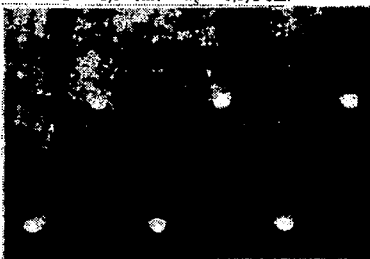


Figure 6h- Spherical segments,
 Plate XIII.

$k = 0.8$ cm; $k = 0.26$ cm;
 $D = 4.0$ cm; $k_s = 0.031$ cm.

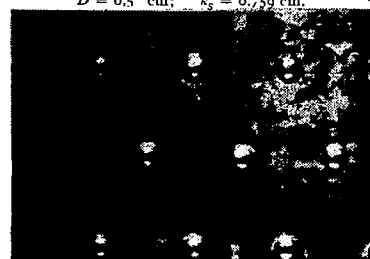


Figure 6i- Spherical segments,
 Plate XIV.

$d = 0.8$ cm; $k = 0.26$ cm;
 $D = 3.0$ cm; $k_s = 0.049$ cm.

Figure 6(a--1).-- Roughness elements of the plates investigated. d = diam. of roughness, D = mean distance of separation of elements; k = height of roughness; k_s = equivalent sand roughness.

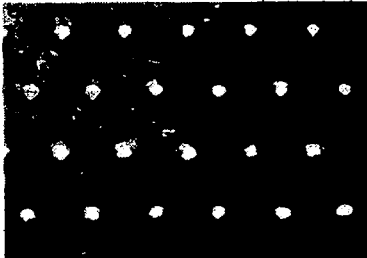


Figure 6k- Spherical segments,
Plate XV.

$d = 0,8 \text{ cm}; k = 0,26 \text{ cm};$
 $D = 2,0 \text{ cm}; k_s = 0,149 \text{ cm}.$

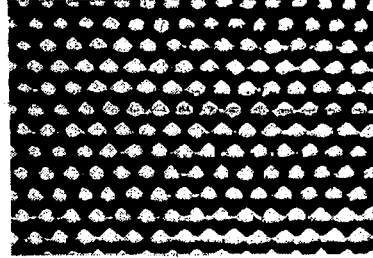


Figure 6l- Spherical segments,
Plate XIX.

$d = 0,8 \text{ cm}; k = 0,26 \text{ cm};$
Closest spacing $k_s = 0,365 \text{ cm}.$

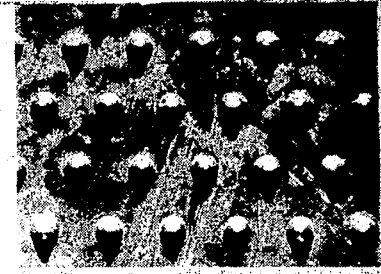


Fig. 6m- Cones, Plate XXIII. Fig. 6n- Cones, Plate XXIV.

Fig. 6o- Cones, Plate XXV.

$d = 0,8 \text{ cm}; k = 0,375 \text{ cm};$
 $D = 4,0 \text{ cm}; k_s = 0,059 \text{ cm}.$

$d = 0,8 \text{ cm}; k = 0,375 \text{ cm};$
 $D = 3,0 \text{ cm}; k_s = 0,164 \text{ cm}.$

$d = 0,8 \text{ cm}; k = 0,375 \text{ cm};$
 $D = 2,0 \text{ cm}; k_s = 0,374 \text{ cm}.$

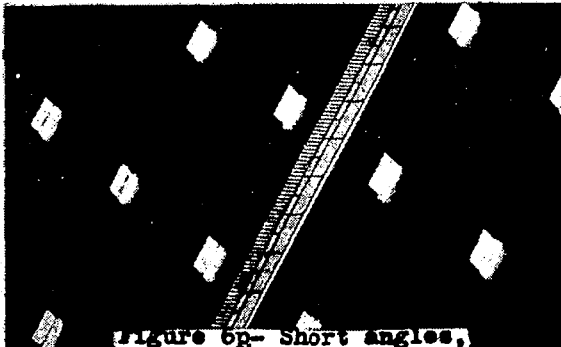


Figure 6p- Short angles,
Plate XVI.

$c = 0,8 \text{ cm}; k = 0,30 \text{ cm};$
 $D = 4,0 \text{ cm}; k_s = 0,291 \text{ cm}.$

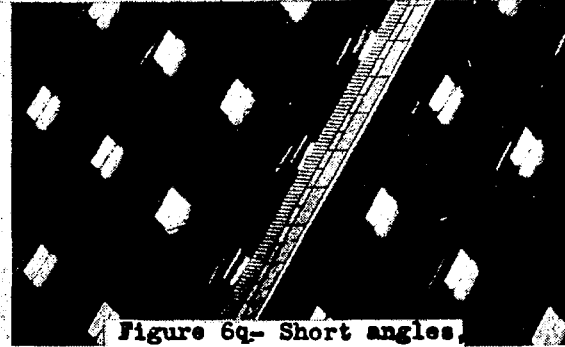


Figure 6q- Short angles,
Plate XVIII.

$c = 0,8 \text{ cm}; k = 0,30 \text{ cm};$
 $D = 3,0 \text{ cm}; k_s = 0,618 \text{ cm}.$

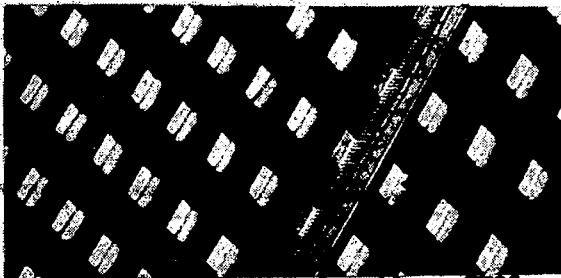


Figure 6r.- Short angles, Plate XVII.
 $c=0.8\text{cm}; k=0.30\text{cm}; D=2.0\text{cm}; k_s=1.47\text{cm}.$

$k=0.135 \text{ cm}; k_s=0.222 \text{ cm}$

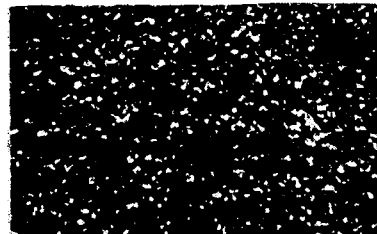


Figure 6s- Hamburg sand, grain size.

Figure 6(k--s).- Roughness elements of the plates investigated. d -diam. of roughness, D -mean distance of separation of elements; k -height of roughness; k_s -equivalent sand roughness.

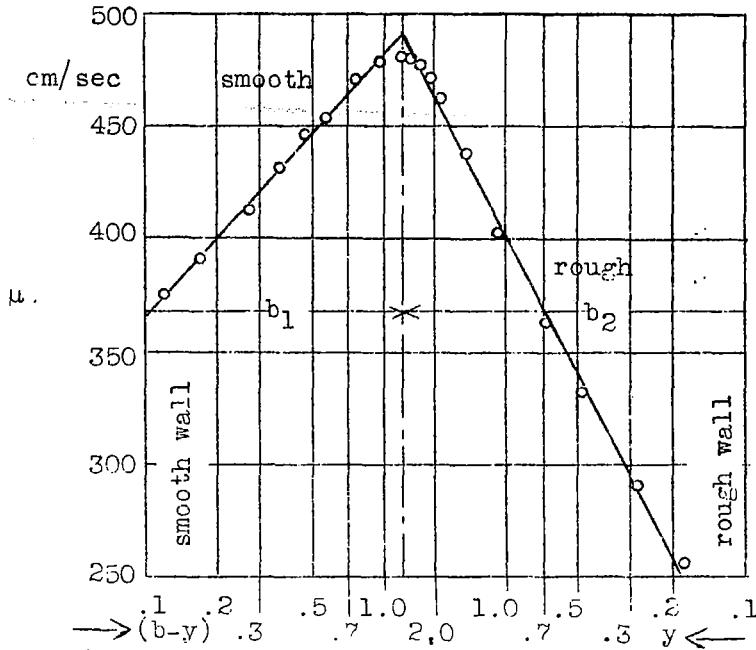


Figure 7.- Nonsymmetrical velocity distribution in channel having smooth and rough walls. Roughness is that of Hamburg sand, $k = 0.135$ cm.

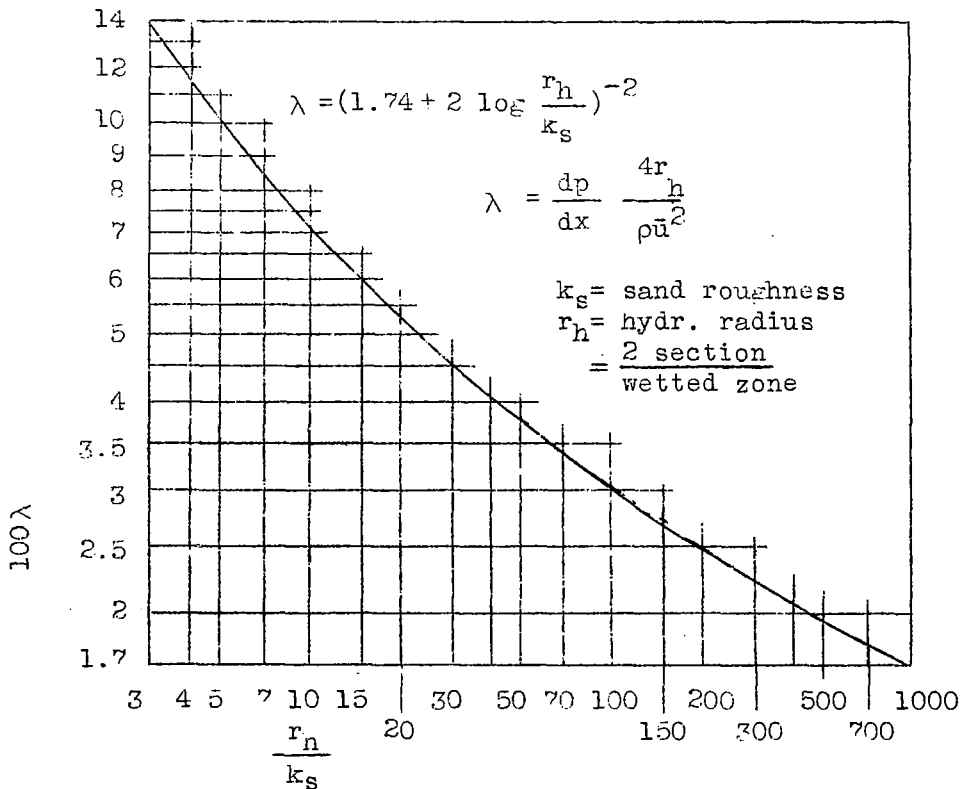


Figure 9.- The resistance factor λ for completely rough flow with sand roughness as a function of the relative roughness r_h/k_s .

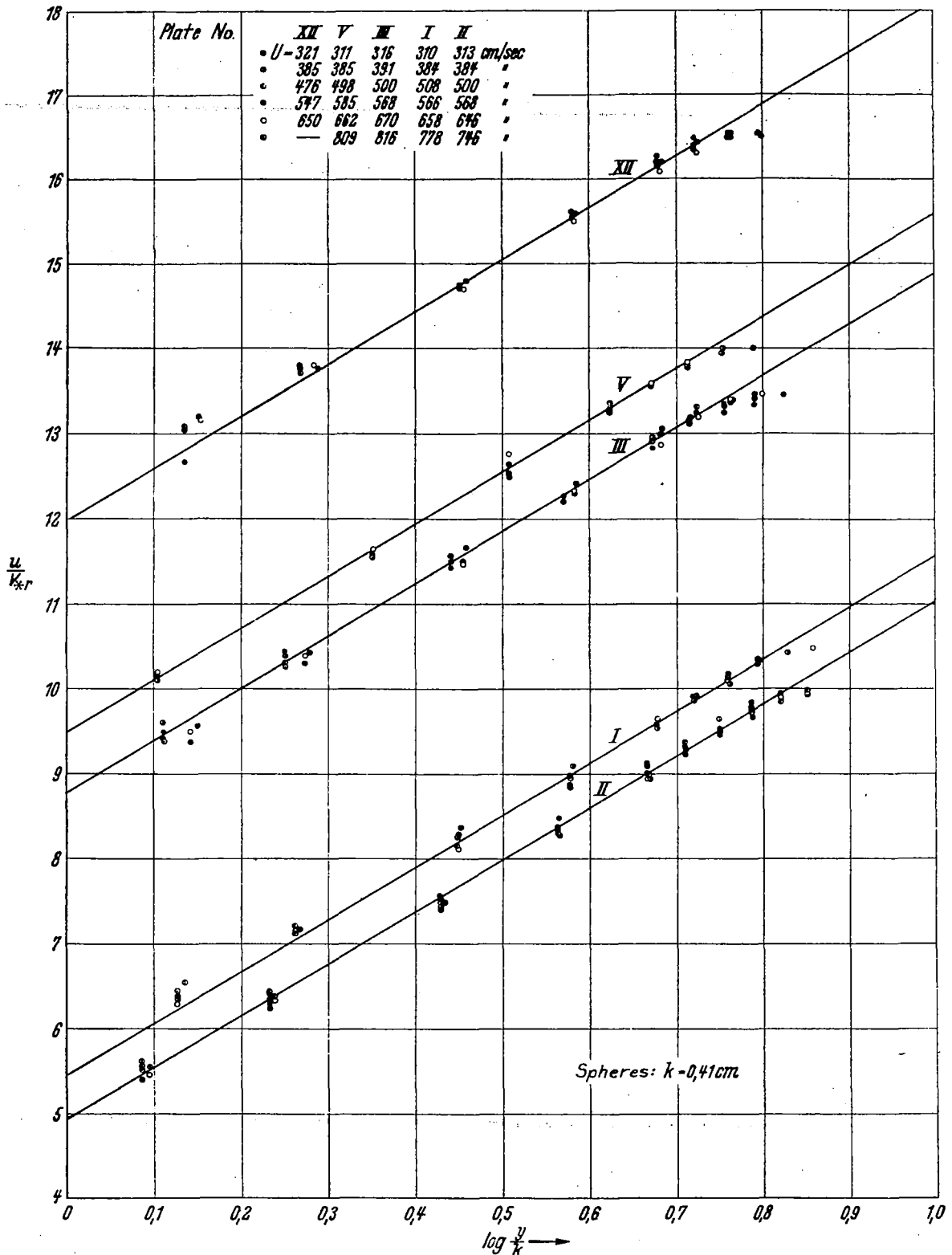


Figure 10.- The nondimensional velocity distribution for the spherical roughness, $d=k=0.41$ cm.

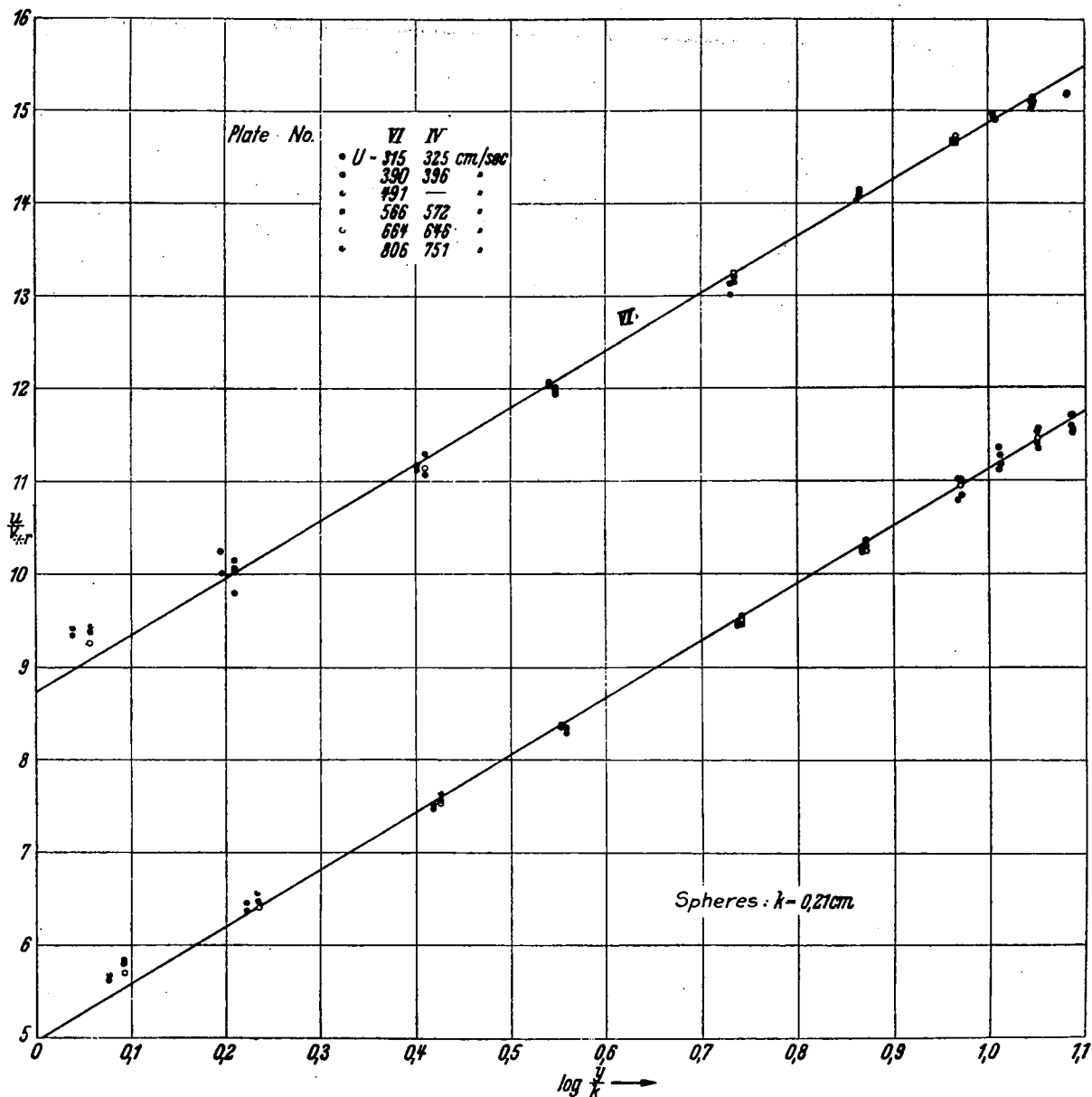


Figure 11.- The nondimensional velocity distribution for the spherical roughness, $d=k=0.21$ cm.

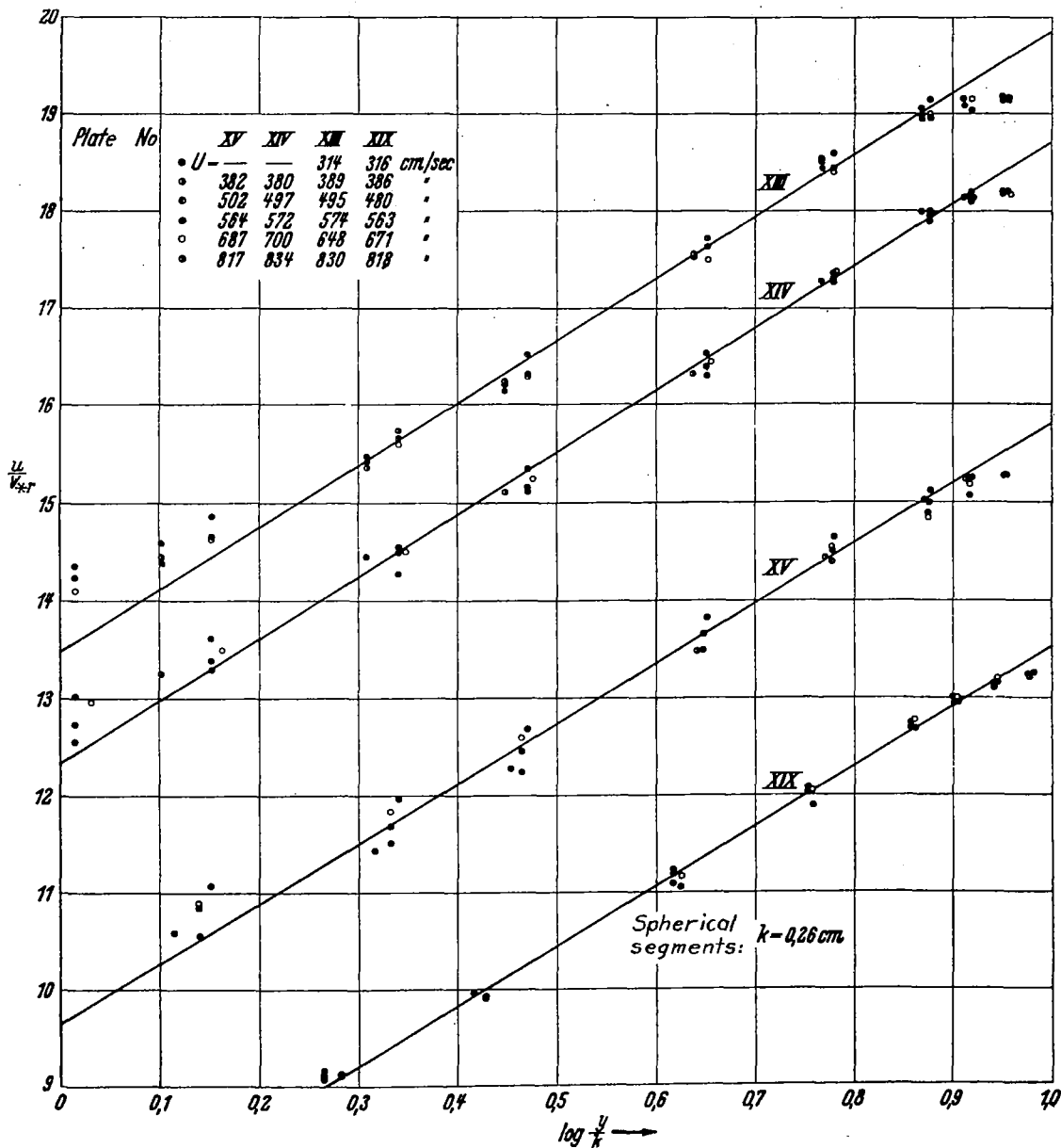
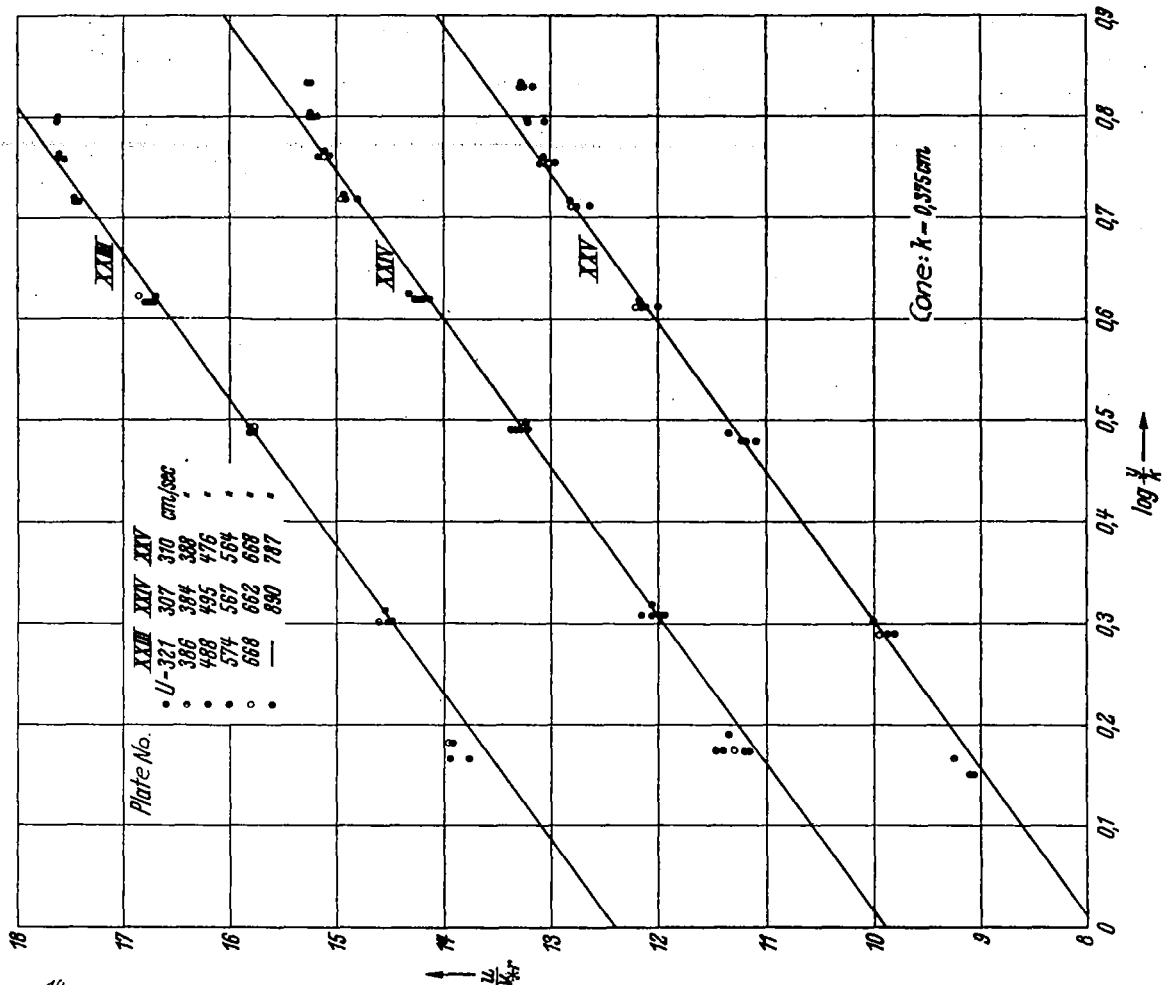


Figure 12.- The nondimensional velocity distribution for the spherical segment roughness, $k=0.26\text{ cm}$.



Cone: $k=0.375\text{cm}$

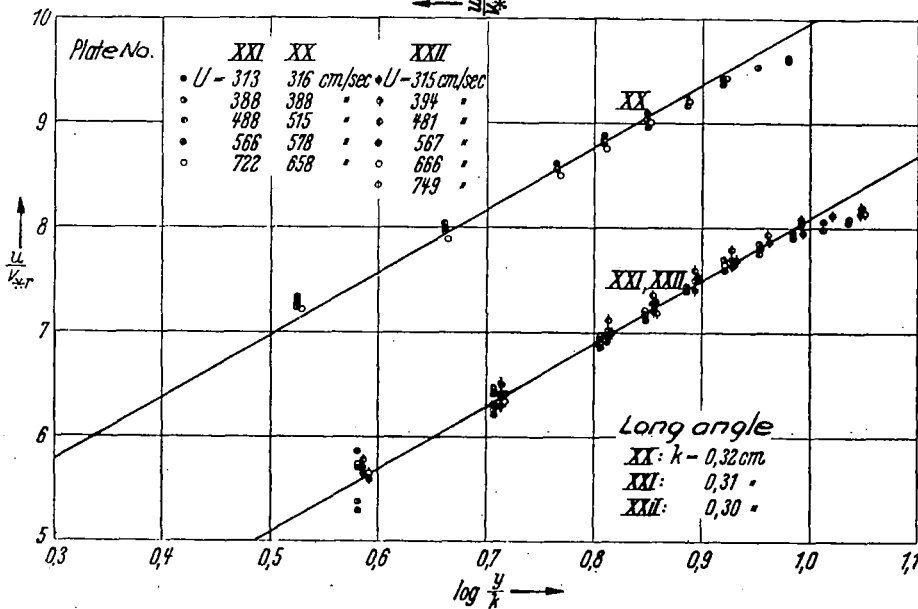


Figure 13.- The nondimensional velocity distribution for the cone roughness, $k=0.375\text{ cm}$.

Figure 15.- The nondimensional velocity distribution for the long angle roughness, $k=0.32, =0.31; =0.30\text{ cm}$.

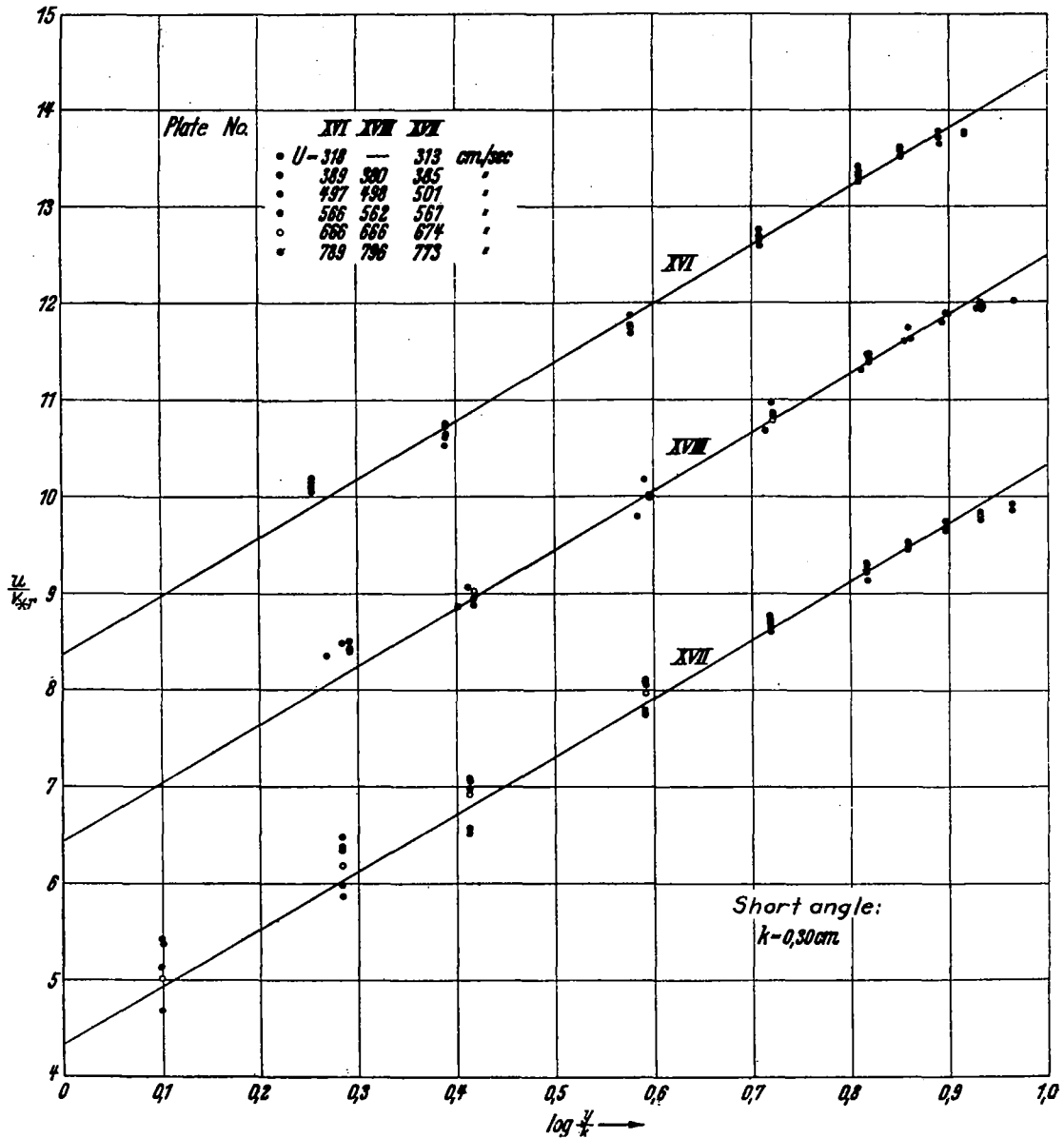


Figure 14.- The nondimensional velocity distribution for the short angle roughness, $k=0.30$ cm.

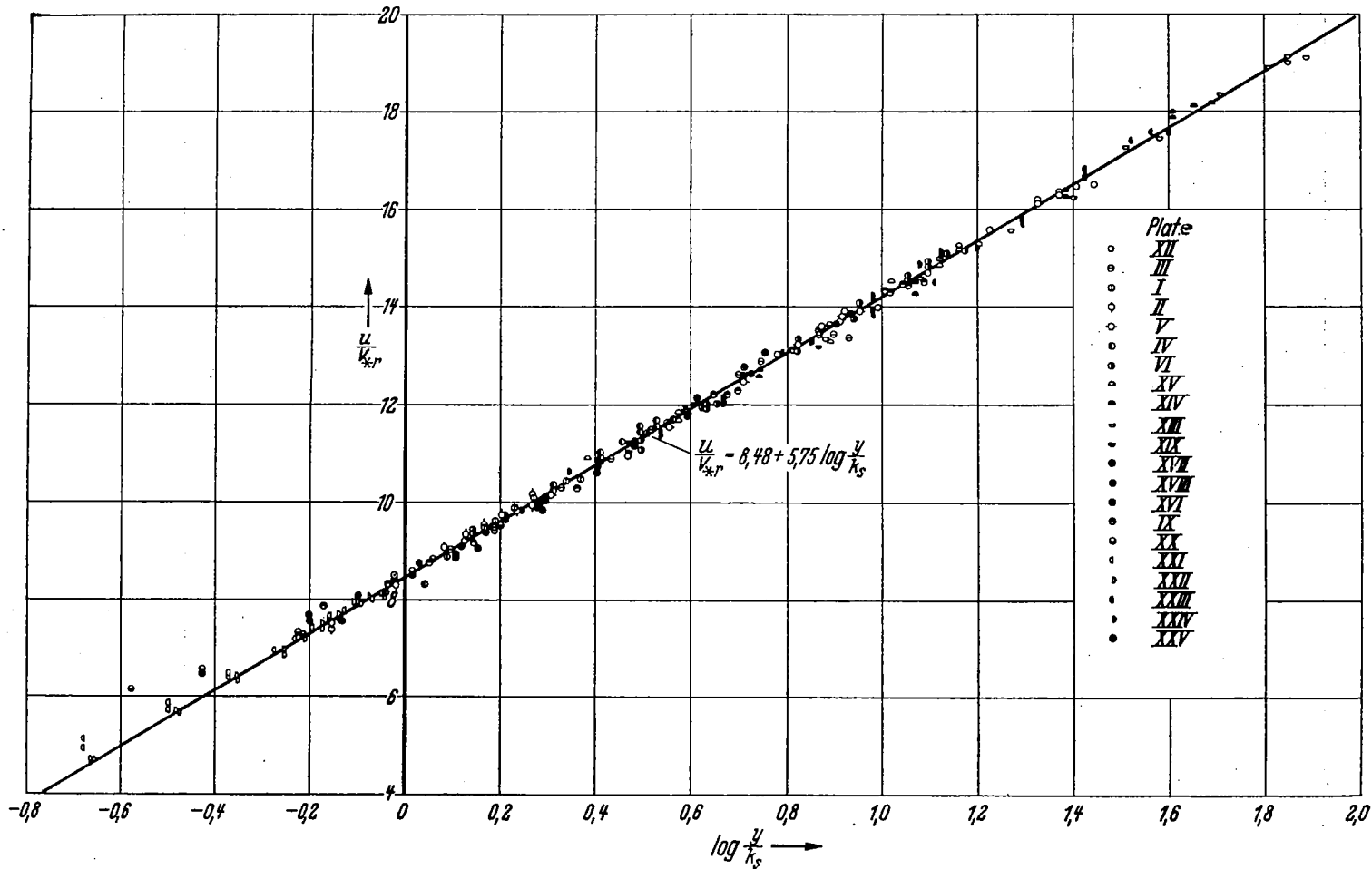
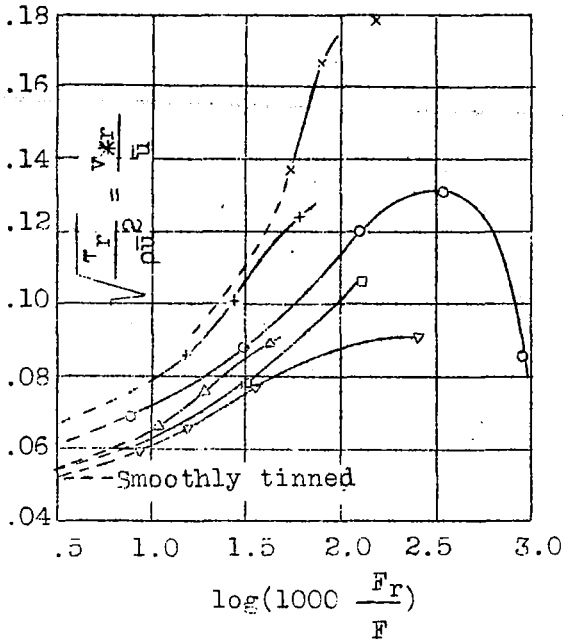


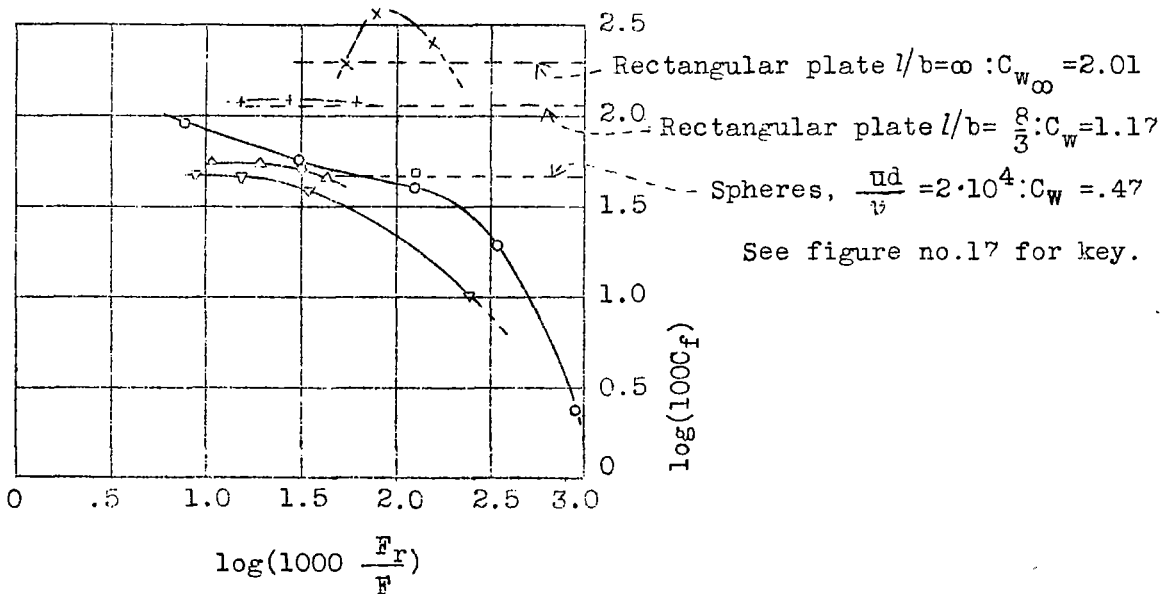
Figure 16.- The velocity distribution for all of the 21 rough plates referred to equivalent sand roughness, plot of u/v_{*r} as a function of $\log y/k_s$.



- Spheres 4.1 mm
- Spheres 2.1 mm
- ▽ Spherical segments
- △ Cones
- + Short angles
- × Long angles

Figure 17.- The dependence of the resistance on the roughness density F_r/F ;

$\sqrt{\frac{\tau_r}{\rho u^2}}$ as a function of $\frac{F_r}{F}$ for sphere, spherical segment, cone, and angle roughness.



See figure no.17 for key.

Figure 18.- The resistance coefficient for the individual roughness element

$C_f = \frac{2W_r}{\rho u_k^2 F_r}$ as a function of the roughness density $\frac{F_r}{F}$.

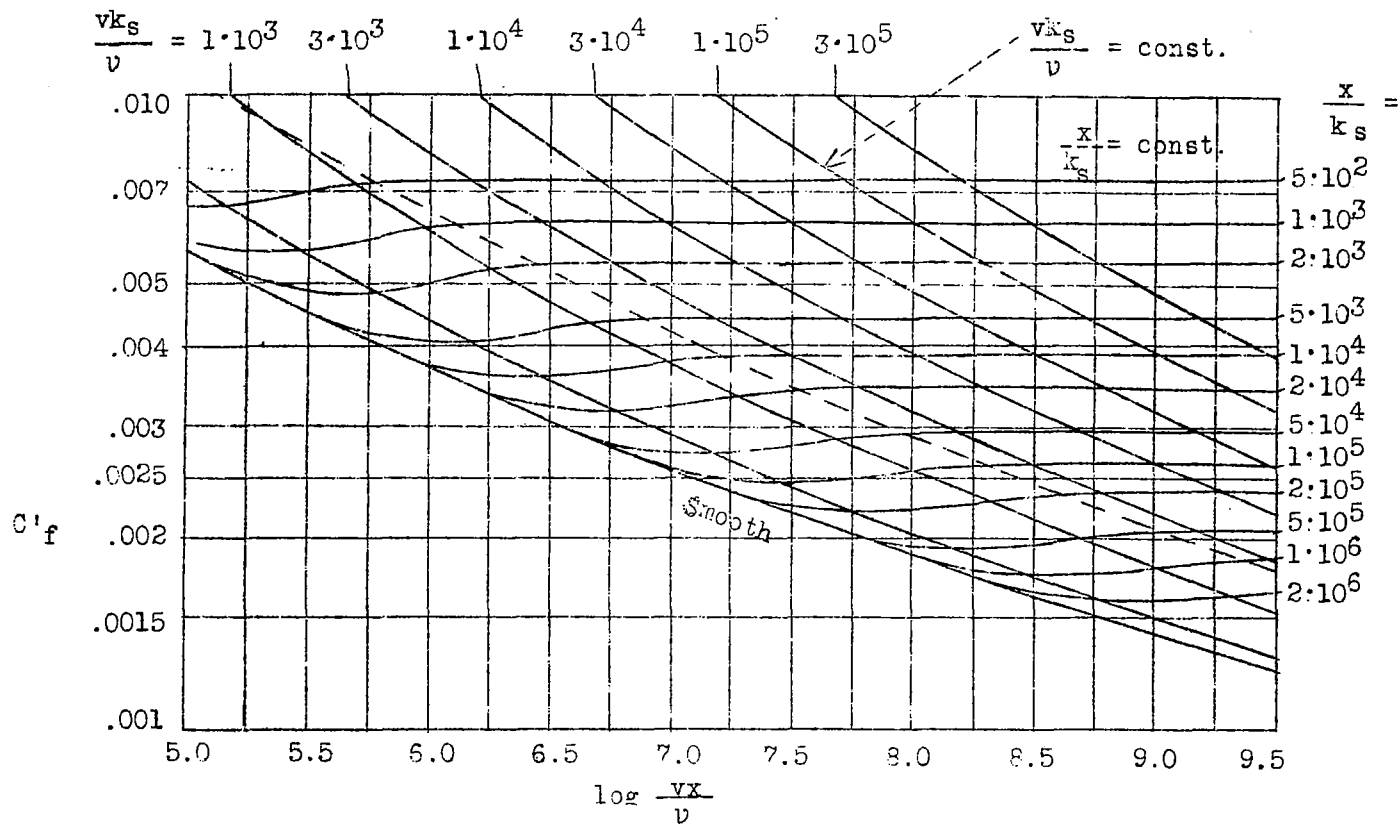


Figure 19.- The local resistance coefficient $C'_f = \frac{2\tau_r}{\rho v^2}$ for rough sand plates as a function of the Reynolds Number $\frac{vx}{v}$ and the relative roughness $\frac{x}{k_s}$, (k_s = sand roughness).

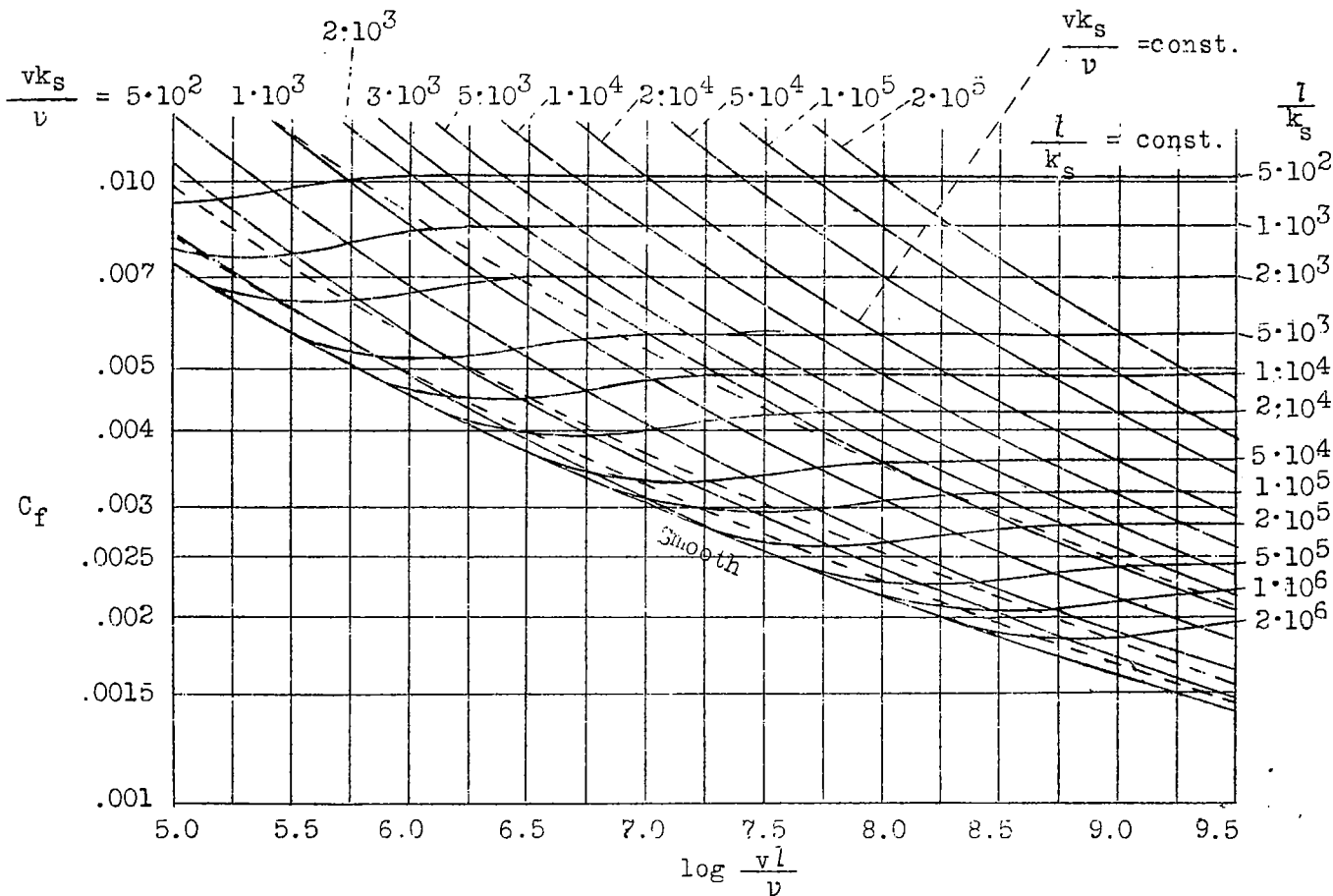


Figure 20.- The total resistance coefficient $C_f = \frac{2W}{\rho v^2 l}$ for rough sand plates as a function of the Reynolds Number $\frac{vl}{\nu}$ and the relative roughness $\frac{l}{k_s}$ (k_s = sand roughness).

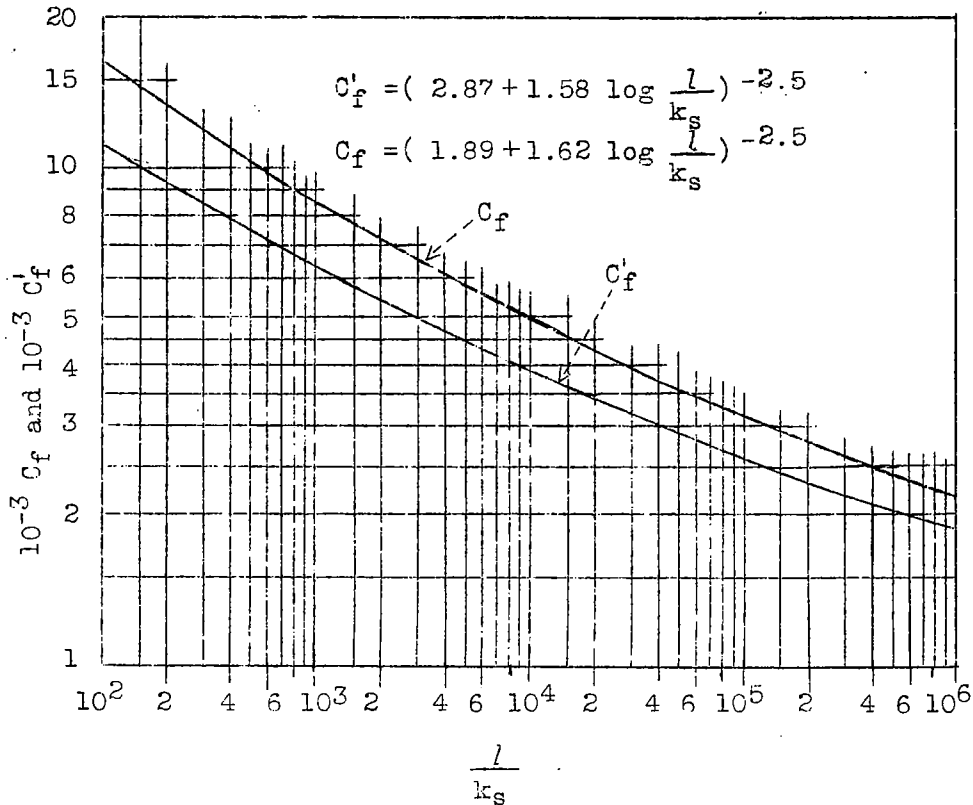


Figure 21.- The total and local resistance coefficients C_f and C'_f for completely rough flow as a function of the relative roughness :

$$\frac{l}{k_s} \left(C'_f = \frac{2\tau}{\rho v^2}, C_f = \frac{2W}{\rho v^2 F} \right).$$

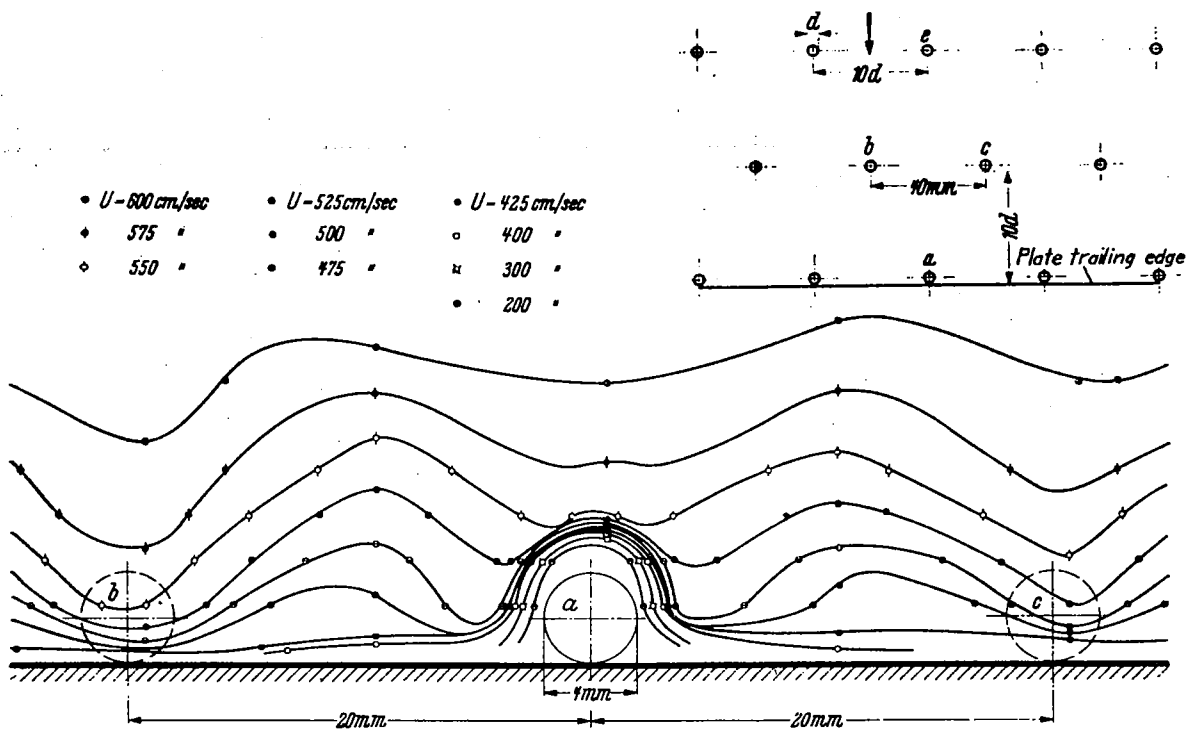


Figure 22.- Lines of equal velocity in plane immediately behind last row of spheres (Plate XII).

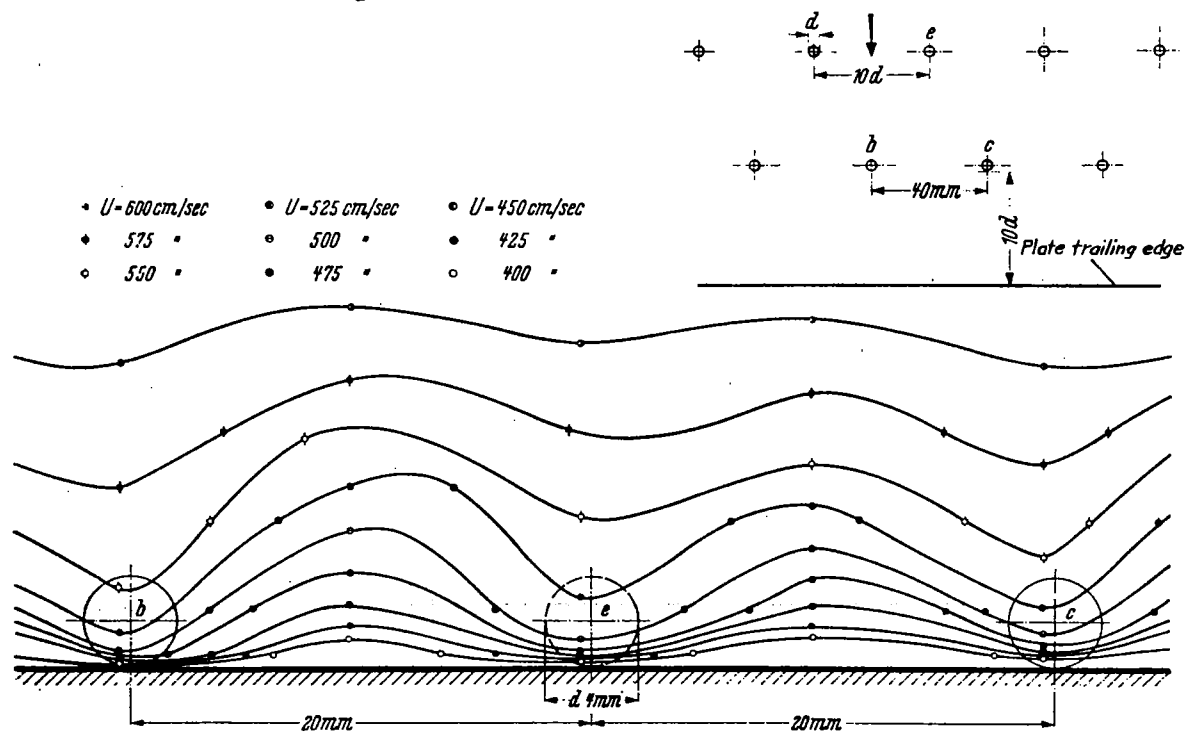


Figure 23.- Lines of equal velocity in plane at distance $10d=4.0$ cm behind last row of spheres (Plate XII).

NASA Technical Library



3 1176 01437 4210